

This file is an uncorrected accepted manuscript (i.e., postprint). Please be aware that this version will change during the production process. This postprint will be removed once the paper is officially published. All legal disclaimers that apply to the journal pertain.

Submitted: 27 July 2025 - Accepted: 17 October 2025 - Posted online: 1 December 2025

To link and cite this article:

doi: 10.5710/AMGH.17.10.2025.3660

PLEASE SCROLL DOWN FOR ARTICLE

- 1 NEW CONTRIBUTIONS TO THE KNOWLEDGE OF ABELISAURIDAE
- 2 (DINOSAURIA, THEROPODA) FROM THE UPPER CRETACEOUS IBERO-
- 3 ARMORICAN LANDMASS.

4

- 5 ERIK ISASMENDI¹, AND ELISABETE MALAFAIA^{2,3}
- 6 ¹Departamento de Geología/Geologia saila, Facultad de Ciencia y Tecnología/Zientzia
- 7 eta Teknologia Fakultatea, Universidad del País Vasco/Euskal Herriko Unibertsitatea,
- 8 Barrio Sarriena s/n, 48940 Leioa, Spain. erik.isasmendi@ehu.eus.
- 9 ²Instituto Dom Luiz, Facultade de Ciências, Universidade de Lisboa, Campo Grande,
- 10 1749-016 Lisboa, Portugal. efmalafaia@ciencias.ulisboa.pt
- ³Grupo de Biología Evolutiva, Facultad de Ciencias, Universidad Nacional de
- 12 Educación a Distancia (UNED), Avenida Esparta s/n, 28323 Las Rozas de Madrid,
- 13 Spain.

14

15 68 pag. (text + references); 9 figs.; 1 table

16

- 17 Running Header: ISASMENDI AND MALAFAIA: ABELISAURID REMAINS FROM
- 18 THE IBERIAN PENINSULA
- 19 Short Description: A revision of theropod remains from Ibero-Armorica, now identified
- 20 as belonging to Abelisauridae, contributes to elucidating abelisaurid paleobiodiversity
- 21 during the Late Cretaceous.

22

23 Corresponding author: Erik Isasmendi. erik.isasmendi@ehu.eus

- 24 **Abstract.** Abelisaurids were medium- to large-bodied theropod dinosaurs that inhabited
- 25 Gondwana and Europe, even becoming the apex predators in the latest Cretaceous
- 26 ecosystems of many of these areas. European abelisaurids remain elusive, but their
- 27 remains are becoming increasingly abundant in the Late Cretaceous deposits of Ibero-
- 28 Armorica. In this work, systematic, morphometric, and cladistic analyses of tooth
- 29 samples from the Campanian–Maastrichian deposits of three localities (Chera 2,
- 30 Montrebei and Viso) from the Iberian Peninsula have allowed these elements to be
- 31 reassigned to abelisaurids. The specimen from Chera 2 is assigned to Arcovenator sp.
- 32 whereas teeth from Montrebei and Viso are classified as Abelisauridae indet. The latter
- 33 represents the first confirmed abelisaurid remain from the Cretaceous of Portugal. The
- 34 axial remains identified as belonging to *Rhabdodon* from the Laño site are here
- 35 attributed to cf. *Arcovenator*. These findings indicate that abelisaurids were the only
- 36 apex terrestrial predators and among the most abundant theropods in the Late
- 37 Cretaceous faunas of the Ibero-Armorican landmass. The reclassification of mid-to
- 38 large-sized isolated teeth from Ibero-Armorica as abelisaurids, rather than
- 39 carcharodontosaurids or closely related forms, suggests that Abelisauridae had already
- 40 become the dominant apex theropod lineage by the Cenomanian. The abelisauroid fossil
- 41 record in Ibero-Armorica spans from the Albian to the latest Maastrichtian, indicating a
- 42 complex and temporally extensive presence. Despite most of the specimens being
- 43 fragmentary, the available evidence supports the persistence and diversification of
- 44 abelisaurids across the Ibero-Armorican domain, with multiple evolutionary lineages
- 45 arising either from a possible Albian stock or resulting from successive dispersals,
- 46 followed by insular diversification throughout the Late Cretaceous.
- 47 **Keywords.** Dinosaur. Ceratosauria. Abelisaurid. Late Cretaceous. Iberian Peninsula.
- 48 Paleobiogeography.

Resumen. NUEVOS APORTES AL CONOCIMIENTO DE ABELISAURIDAE 49 (THEROPODA, DINOSAURIA) DEL CRETÁCICO SUPERIOR 50 51 IBEROARMÓRICANO. Los abelisáuridos fueron dinosaurios terópodos de tamaño 52 medio a grande que habitaron Gondwana y Europa, llegando incluso a convertirse en los 53 depredadores ápice en los ecosistemas del Cretácico final de muchas de estas regiones. 54 Los restos europeos de abelisáuridos siguen siendo limitados, pero sus restos están comenzando a ser más abundantes en los depósitos del Cretácico Superior de Ibero-55 56 Armorica. En este trabajo, los análisis sistemáticos, morfométricos y cladísticos de muestras de dientes del Campaniense-Maastrichtiense de tres localidades (Chera 2, 57 58 Montrebei y Viso) de la Península Ibérica han permitido reasignar estos elementos a 59 Abelisauridae. El espécimen de Chera 2 se asigna a *Arcovenator* sp., mientras que los 60 dientes de Montrebei y Viso se clasifican como Abelisauridae indet. Este último 61 representa el primer resto confirmado de abelisáurido del Cretácico de Portugal. Los 62 restos axiales identificados anteriormente como pertenecientes a Rhabdodon 63 procedentes del yacimiento de Laño se atribuyen aquí a cf. Arcovenator. El registro 64 fósil muestra que los abelisáuridos fueron los únicos depredadores terrestres dominantes 65 y uno de los grupos de terópodos más abundantes en las faunas del Cretácico Superior 66 de Ibero-Armórica. La reclasificación de dientes aislados de tamaño medio a grande 67 como pertenecientes a abelisáuridos, en lugar de a carcarodontosáuridos u otros grupos cercanos, sugiere que Abelisauridae ya se había convertido en el grupo ápice de grandes 68 69 depredadores hacia el Cenomaniense. El registro de abelisauroideos en Ibero-Armórica 70 abarca desde el Albiense hasta el Maastrichtiense final, lo que indica una presencia 71 compleja y prolongada en el tiempo de este grupo de terópodos. A pesar de la naturaleza 72 fragmentaria de la mayoría de los restos, la evidencia apunta a la persistencia y 73 diversificación de los abelisáuridos en el dominio Ibero-Armoricano, con múltiples

- 74 linajes evolutivos surgidos a partir de un posible stock albiense o de dispersiones
- 75 sucesivas, que experimentaron una diversificación a lo largo del Cretácico Tardío en
- 76 Europa.
- 77 **Palabras clave.** Dinosaurio. Ceratosauria. Abelisáurido. Cretácico Tardío. Península
- 78 ibérica. Paleobiogeografía.

79 ABELISAURIDAE comprises medium- to large-bodied (5–9 m in length) ceratosaurian 80 theropods characterized by deep, heavily sculptured skulls with bony protuberances, and 81 short, rounded snouts (Bonaparte, 1991; Wilson et al., 2003; Carrano and Sampson, 82 2008; Canale et al., 2009; Pol and Rauhut, 2012; Cerroni et al., 2022; Amudeo-Plaza et 83 al., 2023). They are recovered as a sister clade to the smaller-bodied Noasauridae within 84 Abelisauroidea (e.g., Novas, 1991; Bonaparte, 1991, 1996; Novas et al., 2013, Baiano et 85 al., 2021). The oldest abelisaurid remains are from the Jurassic of South America and 86 include an isolated abelisaurid tooth from the Late Jurassic of Uruguay (Soto et al., 87 2022) and a relatively complete skeleton of the putative early-branching abelisaurid 88 Eoabelisaurus mefi from the Lower Jurassic of Patagonia (Pol and Rauhut, 2012). 89 Despite being present throughout the Cretaceous of Europe and Gondwana, abelisaurids 90 only became the dominant apex predators after carcharodontosaurids and spinosaurids 91 declined and/or went extinct in the mid Cretaceous (Hendrickx et al., 2015a and 92 references therein). However, they may have been more abundant than other inland 93 predators (Sales et al., 2016). After the Cenomanian-Turonian transition, abelisaurids 94 started to dominate the western European and Gondwanan landmasses (Candeiro and Martinelli, 2005; Carrano et al., 2012; Novas et al., 2013; Tortosa et al., 2014; Csiki-95 96 Sava et al., 2015; Hendrickx et al., 2015a). 97 The European abelisaurid record has significantly increased over the last decades (e.g., Allain and Pereda-Suberbiola, 2003; Buffetaut, 2005; Ősi et al., 2010; Ősi and 98 Buffetaut, 2011; Tortosa et al., 2014; Csiki-Sava et al., 2015; Pérez-García et al., 2016; 99 100 Isasmendi et al., 2022, 2024; Malafaia et al., 2025). The oldest definitive European 101 abelisauroid is currently Genusaurus sisteronis from the Albian of Provence, southern 102 France. Nevertheless, its phylogenetic position remains unresolved, having been 103 recovered as a noasaurid (e.g., Carrano and Sampson, 2008), an early-branching

104 abelisaurid (e.g., Tortosa et al., 2014; Baiano et al., 2023), or a later branching 105 abelisaurid more related to Furileusauria (Buffetaut et al., 2024; Buffetaut, 2025). Caletodraco cottardi is the second abelisaurid from the mid Cretaceous of France. It is 106 107 based on a partial skeleton likely recovered from lower Cenomanian deposits in 108 northwestern France and identified as a furileusaurian brachyrostran (Buffetaut et al., 109 2024). Tarascosaurus salluvicus was the first abelisaurid reported of lower Campanian 110 deposits in southern France (Le Loeuff and Buffetaut, 1991) and despite its fragmentary 111 nature and some authors considering it as a nomen dubium (Rauhut, 2003, Allain and Pereda-Suberbiola, 2003), this taxon was recovered amongst Abelisauridae in the 112 113 phylogenetic analyses performed by Tortosa et al. (2014). Other material from the 114 Iberian Peninsula, such as the Laño femora, have been compared with *Tarascosaurus* 115 (Le Loeuff and Buffetaut, 1991), even though there is no conclusive evidence to support 116 this attribution (Isasmendi et al., 2022; Malafaia et al., 2025). The best-known European 117 abelisaurid is Arcovenator escotae from the upper Campanian of southern France, 118 which has been recovered within Majungasaurinae (Tortosa et al., 2014). The holotype 119 of Arcovenator is composed of a partial skeleton including cranial, axial and 120 appendicular material. Additional isolated teeth and caudal vertebrae from other 121 horizons and areas of the type locality have also been referred to this taxon. 122 Furthermore, other skeletal elements from the Upper Cretaceous of France and the 123 Iberian Peninsula have been assigned to this taxon (Tortosa et al., 2014; Pérez-García et 124 al., 2016; Isasmendi et al., 2022; Malafaia et al., 2025). First regarded as Ceratosauria 125 indet. by Carrano and Sampson (2008), Betasuchus bredai, from Maastrichtian strata of 126 the Netherlands, was finally recovered as an abelisauroid more closely related to 127 Tarascosaurus by Tortosa et al. (2014) and currently represents the latest record of the 128 clade in Europe (Csiki-Sava et al., 2015). Other than abelisaurids, theropod remains

129 from the uppermost Cretaceous Ibero-Armorican mainly belong to small-sized 130 coelurosaurians (e.g., Antunes and Sigogneau-Russell, 1991, 1992; Allain and Taquet, 131 2000; Garcia et al., 2000; Laurent et al., 2002; Laurent, 2003; Ortega et al., 2015; 132 Torices et al., 2015; Marmi et al., 2016; Puertólas-Pascual et al., 2018; Isasmendi et al., 133 2022, 2024; Santos Brilhante et al., 2022; Malafaia et al., 2023) whereas the majority of 134 fossils from large bodied theropods have been either identified as indeterminate 135 theropods (Antunes and Sigogneau-Russell, 1992; Laurent, 2003; Weishampel et al., 136 2004; Company, 2005; Ortega et al., 2015; Torices et al., 2015; Pérez-García et al., 137 2016), tetanurans (Carrano et al., 2012), or ornithomimosaurs (Pereda-Suberbiola et al., 2000). 138 139 This study aims to review the large-bodied theropod material from several uppermost 140 Cretaceous Iberian sites (Chera 2, Laño, Montebrei and Viso), which comprises isolated 141 teeth and some axial elements, including a previously undescribed caudal vertebra. 142 Aside from the systematic studies, morphometric and cladistic analyses were performed 143 on the revised dental elements and the presence of Abelisauridae in Ibero-Armorica is 144 evaluated. 145 146 Institutional abbreviations. DPM, Departamento de Paleontología de Madrid, 147 Universidad Complutense de Madrid, Madrid, Spain; IIPG, Instituto de Investigación 148 en Paleobiología y Geología, General Roca, Argentina; MA, Musée d'Angoulême, 149 Angoulême, France; MACN, Museo Argentino de Ciencias Naturales 'Bernardino 150 Rivadavia', Buenos Aires, Argentina; MAU, Museo Municipal "Argentino Urquiza", 151 Neuquén, Argentina; MCNA, Museo de Ciencias Naturales de Álava/Arabako Natura 152 Zientzien Museoa, Vitoria/Gasteiz, Spain; MG, Museu Geológico, Lisbon, Portugal; 153 MPCA, Museo Provincial Carlos Ameghino, Cipolletti, Argentina; MPCN, Museo

154 Patagónico de Ciencias Naturales, General Roca, Argentina; MPEF, Museo 155 Paleontológico Egidio Feruglio, Chubut, Argentina; MPZ, Museo de Ciencias Naturales de la Universidad de Zaragoza, Zaragoza, Spain; UCPC, Paleontology 156 157 Collection of the University of Chicago, Chicago, USA; UPUAM, Unidad de 158 Paleontología, Universidad Autónoma de Madrid, Madrid, Spain. 159 Anatomical abbreviations. cdl, centrodiapophyseal lamina; cv, cervix; dc, distal 160 carina; dl, dentine layer; dt, denticle; fch, facet for chevron; iet, irregular enamel-161 texture; mc, mesial carina; ns, neural spine; pc, pulp cavity; poz, postzygapophysis; tp, 162 transverse process; **tu**, transverse undulation; **vg**, ventral groove. 163 164 GEOGRAPHICAL AND GEOLOGICAL SETTINGS 165 The skeletal elements here studied were recovered from four Iberian fossil sites namely, 166 Chera 2, Laño, and Montebrei from Spain, and Viso from Portugal. The Chera 2 site is 167 situated near the locality of Chera in the province of Valencia (Valencian Community), 168 about 60 km west of the city of Valencia, in the eastern part of the Iberian Peninsula. 169 The Laño site is located about 30 km south of the city of Vitoria/Gasteiz, in an 170 abandoned sand quarry (the Laño quarry) between the towns of Laño and Albaina 171 (County of Treviño), in the northern Iberian Peninsula. The Montrebei locality is 172 located around 25 km southwest of the Tremp locality, east of the Congost de 173 Montrebei, in the Alsamora municipality (Lleida, northeastern Iberian Peninsula). 174 Finally, the locality of Viso is situated in the Montemor-o-Velho region (Coimbra), at 175 km 20 of the railway (Sauvage 1897–1898), in the western part of the Iberian Peninsula (Fig. 1.1). 176 177 Geologically, the Chera 2 site is located in the Chera Basin (southwestern Iberian 178 Range), specifically in the Sierra Perenchiza Formation (Fm) (e.g., Company, 2005;

179 Company and Szentesi, 2012) (Fig. 1.1). Even though this lithostratigraphic unit reaches 180 a maximum thickness of 300 m, it is only 50 m thick in the Chera area. It comprises 181 lagoonal micritic and brecciated limestones at the base, which transition upwards into 182 palustrine carbonates with evidence of pedogenic alterations towards the top (Platt, 183 1989; Alonso et al., 1991; Company, 2005). This formation has been interpreted as a 184 continental, shallow carbonate environment (Vilas et al., 1982) with shallow, low-185 salinity water bodies at the base (Platt and Wright, 1992) and restricted, ephemeral 186 coastal carbonate lakes and ponds towards the top (Company, 2005). In this context, the 187 Chera 2 site is thought to have formed in an isolated pond that developed in floodplains, 188 where the fossils were transported after high-energy flows (Company, 2005). Peyrot et 189 al. (2020) suggested a late Campanian-?early Maastrichtian age for the Chera site based 190 on palynological studies; however, Company et al. (2005) proposed a late Campanian 191 age for it (Fig. 1.2). 192 The Laño site is located in the Northern Castilian Ramp of the Basque-Cantabrian 193 Basin, specifically on the southern margin of the Miranda-Treviño Syncline (Pereda-194 Suberbiola et al., 2015; Corral et al., 2016) (Fig. 1.1). In the Laño quarry, the Sedano 195 Fm crops out (Berreteaga, 2008; Corral et al., 2016). This formation mainly comprises 196 siliciclastic deposits that can be divided into two units: (1) a lower unit consisting of 197 marine marls and clays and (2) an upper unit composed of silty quartzarenites with 198 interbedded dolomitized limestone layers (Floquet et al., 1982). The Sedano Fm 199 represents a littoral environment, with a siliciclastic sequence in its upper part formed 200 by deltaic aggradation in the subtidal and intertidal areas, prior to the progradation of 201 the delta plain (Corral et al., 2016; Martín-Chivelet et al., 2019). At the Laño quarry, the 202 Sedano Fm is 22 m thick and comprises two different units: (1) the basal unit, which 203 begins with lag deposits of siliciclastic gravel overlain by different sandstone packs

204 with conglomeratic and erosive bases, and (2) the upper unit, which is mainly composed 205 of almost unconsolidated clayey sandstones. The fossils studied herein come from the 206 L1A and L2 vertebrate-bearing beds. Astibia et al. (1990) and Pereda-Suberbiola et al. 207 (2000) interpreted the Laño area as a braided river system, where channels, sandbars 208 and pools developed. Corral et al. (2016) dated the continental vertebrate site of Laño to 209 the late Campanian (chron C32n, 72–73.5 Ma) based on the combination of 210 lithostratigraphic and magnetostratigraphic analyses (Fig. 1.2). 211 The fossil locality of Montebrei is located in the South Pyrenean Basin, precisely in the 212 eastern Tremp Syncline (Fondevilla et al., 2016, 2019) (Fig. 1.1). The latter is the 213 largest of the various sub-basins formed by the compartmentalization of the synform 214 syntectonic sub-basins (Fondevilla et al., 2016). The uppermost Cretaceous and 215 Paleocene lithostratigraphic units crop out in the Tremp Syncline, encompassing 216 marine, transitional, and continental deposits. These include the middle Campanian-217 Maastrichtian Arén Fm and the Maastrichtian-Paleocene Tremp Fm (Mey et al., 1968; 218 Nagtegaal et al., 1983; Mutti and Sgavetti, 1987). The latter overlays and laterally 219 transitions into the Arén Fm (Ardevol et al., 2000; Fondevilla et al., 2016). The Tremp 220 Fm has been informally divided into four units: the 'Grey Garumnian', the 'Lower Red 221 Garumnian', the 'Vallcebre limestones and equivalents', and the 'Upper Red 222 Garumnian' (Rosell et al., 2001; Perez-Pueyo et al., 2021). The Montrebei fossil locality 223 is situated within the 'Grey Garumnian', specifically in La Posa Formation (Torices 224 Hernández, 2002; Torices et al., 2015; Fondevilla et al., 2019). This unit consists of 225 grey marls and mudstones intercalated with sandstones, limestones, and occasional coal 226 beds, containing mixed marine and freshwater invertebrate faunas. It has been 227 interpreted as representing transitional environments such as lagoons, tidal mudflats, 228 and marshes (Eichenseer, 1988; Rosell et al., 2001; Díez-Canseco et al., 2014; Oms et

229 al., 2016). The 'Grey Garumnian' is dated to the latest Campanian-Maastrichtian (Díez-230 Canseco et al., 2014; Vicente et al., 2015, 2016; Fondevilla et al., 2016; Puertolas-231 Pascual et al., 2018) and the Montrebei fossil site dates more precisely to the 'mid' early 232 Maastrichtian (C31r) (Fondevilla et al., 2019) (Fig. 1.2). 233 The vertebrate-bearing site of Viso is found in the Lusitanian Basin, either in the 234 "Sandstones and Mudstones of Viso" of Barbosa et al. (2008) or Viso Fm of Malafaia et 235 al. (2024) (Fig. 1.1). In the latter, a sandstone sequence is predominant, but mudstones, 236 which have been dated to the Campanian–Maastrichtian, based on palynological 237 studies, also crop out (Barbosa et al., 2008) (Fig. 1.2). 238 239 MATERIAL AND METHODS 240 Geographic and stratigraphic context of the material 241 The studied material consists of three isolated teeth from the Chera 2 site (CH 168), 242 Montrebei (DPM-MON-T10 1) and Viso (MG 73), and two vertebrae from the Laño site (MCNA 8366 and 17433). MCNA 8366 comes from the L1A vertebrate-bearing 243 244 bed, and MCNA 17433 was recovered from the L2 fossiliferous level. The specimens 245 are in three separate institutions namely, the Universidad Complutense de Madrid of 246 Spain (DPM-MON-T10 1), Museu Geológico of Lisbon, Portugal (MG 73), and the 247 Arabako Natura Zientzien Museoa/Museo de Ciencias Naturales de Álava of Vitoria-248 Gasteiz, Spain (MCNA 8366 and 17433). The tooth CH 168 was studied based on 249 photographs and a cast. 250 Historically, DPM-MON-T10 1 was considered as the tooth of an indeterminate 251 theropod by Torices et al. (2015), before being assigned to an indeterminate 252 Abelisauridae by Isasmendi et al. (2024). It should be noted that this specimen never 253 received a proper description. The tooth MG 73 was first attributed to *Megalosaurus* sp.

by Sauvage (1897–1898) at the end of the 19th century, then to Megalosaurus cf. 254 255 pannoniensis by Lapparent and Zbyszewski (1957), and recently to Theropoda indet. by 256 Malafaia et al. (2024). The neural arch MCNA 8366 was originally assigned to 257 Rhabdodon by Pereda-Suberbiola and Sanz (1999), while the vertebra MCNA 17433 258 (previously labeled as MCNA 14077) was tentatively identified as Abelisauridae indet. 259 by Isasmendi et al. (2021). Finally, the tooth CH 168 was referred to as Theropoda 260 indet, by Company (2005), as ?Neoceratosauria indet, by Company et al. (2009) and as 261 cf. Arcovenator by Isasmendi et al. (2022). Comparative methodology and terminology for the isolated teeth. Unlike the 262 263 postcranial remains, which was studied first-hand, the isolated teeth were studied under 264 a stereo microscope (Nikon® SMZ645) and through first-hand observations. Crown-265 based measurements were taken using a digital caliper (Juning®), while denticle-based 266 measurements were taken either under the stereo microscope or with the Imagej 267 software (v.1.51j8). The study of the isolated teeth follows the anatomical, positional, 268 directional and morphometric nomenclature proposed by Smith and Dodson (2003), 269 Smith et al. (2005), and Hendrickx et al. (2015b). 270 Measurements taken on the isolated teeth. The following measurements were taken 271 on the studied sample based on Currie et al. (1990), Smith et al. (2005), and Hendrickx 272 et al.'s (2015b, 2020) methodology (see Supplementary material 1): crown base length 273 (CBL), crown base width (CBW), mid-crown length (MCL), mid-crown width (MCW), crown height (CH), apical length (AL), extent of the mesiobasal denticles 274 275 (MDE), length of the mesial serrated carina (MSL), distoapical denticle density (DA), 276 distobasal denticle density (**DB**), distocentral denticle density (**DC**), mesical 277 denticle density (MA), mesiobasal denticle density (MB), mesiocentral denticle density (MC), mesial denticle length (MDL), and distal denticle length (DDL). In addition, the 278

- 279 crown base ratio (CBR; as CBW/CBL), crown height ratio (CHR; as CH/CBL), mid-
- 280 crown ratio (MCR; as MCW/MCL), mesial angle of the crown (CMA), distal angle of
- crown (CDA), average mesial denticle density (MAVG; as (MA+MC+MB)/3),
- average distal denticle density (**DAVG**; as (DA+DC+DB)/3), and denticle size density
- index (**DSDI**; as MC/DC) were calculated. The MCA and DCA were calculated using
- 284 the following equation (Smith, 2007; Serrano-Martínez et al., 2015):

285
$$CMA = arcos \frac{CBL^{-2} + AL^{-2} - CH^{-2}}{2 \times CBL \times AL}$$
 and $CDA = arcos \frac{CBL^{-2} + CH^{-2} - AL^{-2}}{2 \times CBL \times AL}$

- 286 Linear discriminant analyses (LDA) on the isolated teeth. The classification of the
- 287 isolated teeth was supported by several linear discriminant analyses performed using
- 288 PAST v.4.05 (Hammer et al., 2001). When performing the LDAs, variables expressed
- as ratios (CBR, CHR and MCR) as well as the crown angles (CDA and CMA) were
- 290 excluded, as these are not independent but weighted variables (Hendrickx et al., 2015b).
- 291 Furthermore, to ensure that all variables were metric-based, measurements of denticle
- length (MLD and DDL) were used instead of denticle densities, in accordance with the
- approach of Hendrickx et al. (2020). Following Malafaia et al. (2025), the number of
- 294 flutes on the labial and lingual surfaces (**LAF** and **LIF**, respectively) were not included
- in the analyses, as there are non-metric variables. Therefore, a total of 10 variables were
- used in the performed LDAs, as Malafaia et al. (2025). These variables are: CBL, CBW,
- 297 CH, AL, MCL, MCW, MDE, MSL, MDL, and DDL. To perform the LDAs, the
- 298 database and a similar methodology proposed by Malafaia et al. (2025) were used (see
- 299 Supplementary material 1). Prior to conducting the morphometric analyses, the data
- were normalized using a Log (x+1) transformation for all variables to avoid zero values.
- 301 In addition, as proposed by Young et al. (2019) and Hendrickx et al. (2020), an arbitrary
- 302 value of 100 denticles per five millimeters was used for those specimens with non-
- 303 denticulated carinae. Finally, specimens studied herein were not assigned to any

304 predefined group for the LDAs and were instead treated as belonging to an "unknown 305 taxon". 306 Firstly, two linear discriminant analysis, one at the taxon level and another at the clade 307 level, were carried out using a database comprising 528 teeth with the data from 308 Hendrickx et al. (2020) (Database 1; Supplementary material 1) belonging to twenty-309 four Cretaceous taxa (twenty-two genera, and two indeterminate family-level clades), 310 with the aim of minimizing potential noise (see Malafaia et al., 2025; Supplementary 311 material 1). This dataset gathers dental measurements from one non-abelisauroid ceratosaurian (Genyodectes), nine abelisaurids (Abelisaurus, Arcovenator, Aucasaurus, 312 313 Carnotaurus, Chenanisaurus, 'Indosuchus', Majungasaurus, Skorpiovenator, and 314 Abelisauridae indet.), three spinosaurids (*Baryonyx*, *Suchomimus* and Spinosaurinae 315 indet.), one neovenatorid (*Neovenator*), two megaraptorans (*Australovenator* and 316 Fukuiraptor), five carcharodontosaurids (Acrocanthosaurus, Carcharodontosaurus, 317 Eocarcharia, Giganotosaurus, and Mapusaurus), and six tyrannosaurids 318 (Albertosaurus, Alioramus, Daspletosaurus, Gorgosaurus, Tyrannosaurus and 319 Zhuchengtyrannus). 320 Afterwards, two additional LDAs were performed, one at taxon level and another at 321 clade level, excluding the groups that plotted well-separated from the herein studied 322 teeth (Database 2; Supplementary material 1), as these were considered not closely 323 related. The excluded specimens belonged to all spinosaurids, as well as the 324 tyrannosaurids Daspletosaurus, Tyrannosaurus and Zhuchengtyrannus, and the 325 carcharodontosaurid Carcharodontosaurus. 326 Finally, a fifth LDA was performed with the third database (Database 3; Supplementary 327 material 1) compiled by Malafaia et al. (2025), which includes Ibero-Armorican 328 abelisaurids or specimens classified among Abelisauridae. These consist of the

329 indeterminate abelisaurids from the Western Tremp Syncline (South Pyrenean Basin) 330 (Isasmendi et al., 2024), the abelisaurid teeth closely related to Arcovenator from Poyos 331 (Malafaia et al., 2025), the specimens referred to cf. Arcovenator from Armuña (Pérez-332 García et al., 2016), and the Arcovenator specimens from Jas Neuf Sud and Laño 333 (Tortosa et al., 2014; Hendrickx et al., 2020; Isasmendi et al., 2022). In this analysis, the isolated teeth of an indeterminate tetanuran from Iharkút (Ősi et al., 2010) were 334 335 excluded from the dataset. 336 **Cladistic analysis.** A cladistic analysis was performed based on the dentition-based 337 matrix (146 morphological dental characters) of Hendrickx et al. (2020), into which we 338 scored the isolated teeth MG 73, CH 168, and DPM-MON-T10 1 (see Supplementary 339 material 2). The positive constraints defined by Hendrickx et al. (2020) were applied in 340 these analyses to recover a topology consistent with the most recent phylogenetic 341 hypotheses. Additionally, to test the phylogenetic affinities of the studied specimens 342 within the Abelisauridae clade, we constrained their placement and evaluated the 343 additional steps required to achieve that position. The phylogenetic analysis was carried 344 out using TNT 1.6 (Goloboff and Morales, 2023). The studied specimens were scored 345 using Mesquite 3.7 (Maddison and Maddison, 2011) and subsequently imported into 346 TNT. The search strategy follows the protocol used by Hendrickx et al. (2020), 347 beginning with a combination of the tree-search algorithms, including Wagner trees, 348 TBR branch swapping, sectorial searches, Ratchet (with the perturbation phase stopped 349 after 20 substitutions), and Tree Fusing (5 rounds), until 100 hits of the same minimum 350 tree length were achieved. The best trees recovered were subjected to a final round of 351 TBR branch swapping. Zero-length branches in any of the recovered most parsimonious 352 trees were collapsed. Consistency (CI) and retention (RI) indexes were obtained using 353 the STATS.RUN command.

354	
355	SYSTEMATIC PALEONTOLOGY
356	Suborder THEROPODA Marsh, 1881
357	Infraorder CERATOSAURIA Marsh, 1884
358	Family ABELISAURIDAE Bonaparte and Novas, 1985
359	Abelisauridae indet.
360	Figure 2
361	Morphotype 1
362	Referred material. DPM-MON-T10 1, one isolated mesial tooth (Fig. 2.1–2.7).
363	Geographic occurrence. Montrebei (Lleida, Spain).
364	Stratigraphic occurrence. 'Grey Garumnian' strata of the Tremp Formation; La Posa
365	Formation; 'mid' early Maastrichtian (C31r) (Torices Hernández, 2002; Torices et al.,
366	2015; Fondevilla et al., 2019).
367	Description. DPM-MON-T10 1 consists of a crown that lacks its basal portion and the
368	apex (Fig. 2.2–2.5). It is here interpreted as a mesial tooth, based on its symmetrical
369	'D'-shaped cross-section, relatively thick crown, and asymmetrical labial and lingual
370	surfaces (Hendrickx et al., 2015b, 2020). No denticles are complete, but the bases of the
371	mesial denticles and some distal denticle bases are preserved (Fig. 2.1). The enamel is
372	also largely missing, but a patch is preserved on the mesioapical part of the labial
373	surface (Fig. 2.6). The crown is ziphodont, not very compressed labiolingually and quite
374	distally curved, with its apicalmost part extending beyond the basodistalmost point of
375	the crown (Fig. 2.2–2.5). The mesial margin of the crown is strongly convex, and the
376	distal margin is concave in lateral view (Fig. 2.5). In distal view, the labial surface is

- 377 convex, and the lingual one is mostly straight, making the crown slightly lingually tilted
- 378 (Fig. 2.4). The lingual and labial surface are convex, but the lingual surface becomes
- 379 flatter close to the distal carina. The basalmost cross-section of the preserved crown is
- nearly subsymmetrical 'D'-shaped, whereas the mid cross-section is lanceolate (Fig.
- 381 2.7).
- 382 Both mesial and distal carinae are present and denticulated, but because the basal part of
- 383 the crown is not preserved, their entire extension cannot be assessed. The mesial carina
- is mesiolingually oriented and straight; it is centered apically but slightly displaces
- lingually toward the base (Fig. 2.2). On the other hand, the distal carina is straight and
- strongly labially deflected (Fig. 2.4). The mesial denticle density is 10 denticles per five
- 387 mm apically and at mid crown and there is no random variation of denticle-size.
- 388 The preserved enamel surface is slightly polished and exhibits micro-scratches. The
- enamel-texture is subtle, non-oriented, and irregular (Fig. 2.6).
- 390 Morphotype 2
- 391 **Referred material.** MG 73, one isolated lateral tooth (Fig. 2.8–2.12).
- 392 **Geographic occurrence.** Viso locality, region of Montemor-o-Velho, Coimbra, Portugal
- 393 (Sauvage, 1897-1998; Malafaia et al., 2024).
- 394 **Stratigraphic occurrence.** Viso Formation (also known as Sandstones and Mudstones
- of Viso); Campanian–Maastrichtian (Barbosa et al., 2008; Malafaia et al., 2024).
- 396 **Description.** MG 73 consists of a lateral tooth crown that lacks the apex and a fragment
- of the root (Fig. 2.8–2.12). It is interpreted as a lateral tooth based on its symmetrical
- 398 cross-section outline and low CBR value (see Hendrickx et al., 2015b, 2019, 2020). The
- enamel layer is eroded on its lingual surface (Fig. 2.11), and the mesial carina is almost
- 400 entirely abraded (Fig. 2.8). The distal carina is also poorly preserved but the bases of the

401 denticles are visible along the carina and the basal denticles are relatively well 402 preserved (Fig. 2.10–2.11). 403 This crown is relatively elongate, ziphodont, and strongly labiolingually flattened (Fig. 404 2.8–2.12), with a CBR of 0.58 (CBL=12 mm and CBW=7 mm). The crown is distally 405 curved, but it is not possible to determine whether the apex would have extended 406 beyond its basodistalmost point (Fig. 2.11). In lateral view, the mesial margin is convex, 407 while the distal margin is slightly concave, becoming straighter toward the base (Fig. 408 2.11). In distal view, the lingual surface is slightly concave, and the labial surface is 409 convex, suggesting that the apex was slightly tilted lingually (Fig. 2.10). There is no 410 concave surface adjacent to the carinae, but the lingual surface becomes flat near the 411 distal carina (Fig. 2.9). The basal cross-section of the crown is lanceolate (Malafaia et 412 al., 2024) and the cross-section of the root is oval (Fig. 2.12). No basal constriction is 413 present between crown and root. 414 The distal carina reaches the cervix and the distal denticles are present along the entire 415 preserved length (Fig. 2.10). Denticles also appear to be present on the mesial carina, 416 but only their bases are visible at mid-crown (Fig. 2.8). The full extent of the mesial 417 carina cannot be determined (Malafaia et al., 2024). The distal carina is centrally located 418 and slightly bowed whereas the mesial carina is more lingually positioned and straight 419 (Fig. 2.8 and 2.10). There is no random variation in denticle size along the distal carina 420 and the denticles decrease in size towards the base. Only the distal denticle densities 421 could be measured. The DC value is 20 denticles per five millimeters, and the DB is 422 22.5 denticles per five millimeters. The basal denticles are sub-quadrangular with 423 slightly convex external margins and are separated by narrow interdenticular spaces. 424 The denticles are poorly preserved at mid-crown, with only the bases of some visible. 425 These are also separated by narrow interdenticular spaces and seem slightly longer

426 apicobasally than mesiodistally. However, because the external end is not preserved, 427 this morphology cannot be confirmed. Interdenticular sulci are not visible adjacent to 428 either the distal or mesial carinae. Some subtle transverse undulations are present on the 429 enamel of the lingual surface of the crown (Fig. 2.9). The enamel texture is subtle, non-430 oriented, and irregular (Malafaia et al., 2024). 431 Genus Arcovenator Tortosa, Buffetaut, Vialle, Dutour, Turini and Cheylan, 2014 432 Cf. Arcovenator sp. 433 Figure 3–4 434 Referred material. MCNA 8366, an anterior dorsal vertebra; MCNA 17433, an anterior 435 to middle caudal vertebra. 436 Geographic occurrence. Laño site, Treviño County, Spain. 437 Stratigraphic occurrence. Sedano Formation; upper Campanian (C32n) (Corral et al., 438 2016). 439 Description. 440 Axial skeleton. 441 **Dorsal vertebra** (Fig. 3.1–3.4). MCNA 8366 comprises the neural arch of an anterior 442 dorsal vertebra (probably a D1 or D2, based on O'Connor, 2007). This neural arch is 443 covered by an iron patina and lacks both prezygapophyses (Fig. 3.1–3.4). The neural 444 spine and the left transverse process are badly damaged, with only their bases preserved. 445 The right transverse process is laterally projected and horizontal but slightly inclined 446 anteriorly, forming an angle of less than 20° relative to the horizontal plane (Fig. 3.1– 447 3.4). It measures 46 mm in length and is developed in the anterior half of the vertebra. 448 In dorsal view, the right transverse process expands anteroposteriorly towards the 449 diapophysis, making it fan-shaped in this view (Fig. 3.4). The posterior edge of the

450 transverse process is straight, and its anterior margin is convex. In lateral view, the 451 diapophysis is D-shaped and faces ventrolaterally (Fig. 3.2). The base of the neural 452 spine is mediolaterally narrow anteriorly and broadens posteriorly. It extends posteriorly 453 beyond the bases of the prezygapophyses, almost reaching the posterior margin of the 454 postzygapophyses (Fig. 3.4). The postzygapophyses face ventrolaterally, are subcircular 455 in outline, and appear to overhang the centrum (Fig. 3.1 and 3.2). The presence or 456 absence of a hyposphyene-hypantrum articulation cannot be determined (Fig. 3.1). 457 Caudal vertebrae (Fig. 3.5–3.8). MCNA 17433 consists of the centrum and the base of 458 the neural arch of an anterior to middle caudal vertebra (posterior to C5 due to its 459 straighter anterior and posterior margins, based on Méndez, 2014), which are slightly 460 mediolaterally compressed due to deformation (Fig. 3.5–3.8). The centrum and neural 461 arch are almost fully fused, with the suture line being almost indiscernible (Fig. 3.7). 462 The centrum is amphicoelous, spool-shaped, and slightly elongated (Fig. 3.5–3.8). 463 MCNA 17433 measures 79 mm in anteroposterior length. Its anterior articular surface is 464 57 mm in height and 46 mm in width, while the posterior articular surface is 64 mm in 465 height and 46 mm in width. Both the anterior and posterior articular surfaces are 466 elliptical (Fig. 3.6 and 3.8). In lateral view, the anterior and posterior surfaces are 467 straight, and the ventral margin is concave (Fig. 3.7). The centrum is medially 468 compressed and exhibits relatively shallow pleurocentral depressions. However, the 469 base of the neural arch is wider than the mid-centrum. The ventral surface of the 470 centrum features an anteroposterior longitudinal groove, which is laterally delimited by 471 a ridge on each side (Fig. 3.5). In the same view, the posterior end of the centrum 472 exhibits quite prominent facets for articulation with the haemal arches, making the 473 posterior end of the centrum more ventrally projected (Fig. 3.5).

The preserved portion of the neural arch includes the bases of the transverse processes

(Fig. 3.5 and 3.7), which are centrally located and ventrally positioned in the neural

arch. These processes are relatively thin and sheet-like and the preserved parts taper

laterally. The ventral surface of the left transverse process exhibits a possible broad but

not very protruding centrodiapophyseal lamina (Fig. 3.5 and 3.7).

479 Arcovenator sp.

480 Figure 4

- **Referred material.** CH 168, one isolated lateral tooth.
- **Geographic occurrence.** Chera, Valencia, Spain.
- **Stratigraphic occurrence.** Sierra Perenchiza Formation; upper Campanian (Company,
- 484 2005; Company et al., 2005).

Description. CH 168 preserves the crown and part of the root. It is interpreted as a lateral tooth based on its symmetrical cross-section outline and low CBR value (see Hendrickx et al., 2015b, 2019, 2020). The base of the crown is distally damaged, and fractures are present throughout the crown (Fig. 4). Parts of the carinae are also missing. An apically located elliptical wear facet is present on the labial surface (Fig. 4.5). The crown is ziphodont, labiolingually compressed, and distally curved. The apex extends slightly beyond the basodistalmost point of the crown (Fig. 4). In lateral view, the mesial margin is convex, while the distal margin is concave apically, becoming straighter toward the base (Fig. 4.3 and 4.5). In distal view, the lingual surface is straight basally and convex apically whereas the labial margin is convex basally and becomes straighter apically (Fig. 4.4). Both labial and lingual surfaces are convex, with no concave surfaces adjacent to any carinae. The lingual margin becomes more planar

near the base of the distal carina. The basal cross-section of the crown is oval to

498 lanceolate (Fig. 4.6), and the mid cross-section is lenticular. The cross-section of the 499 root is more oval, with no basal constriction between the root and the crown. The CBL measures 15.47 mm, whereas the CBW measures 9.88 mm, resulting in a 500 501 CBR of 0.64. The CH is 30.02 mm, being the CHR of 1.94. The AL measures 33.52 502 mm. 503 Both mesial and distal carinae are denticulated (Fig. 4.1 and 4.8). The mesial carina is 504 straight, centered apically and mesiolingually displaced toward the base of the crown. 505 The mesial carina does not reach the cervix but extends from the apex to approximately 506 two-thirds of the crown (Fig. 4.2). The distal carina reaches the cervix, and it is 507 sigmoidal in distal view and labially deflected (Fig. 4.4). 508 The denticles are largest at mid-crown on the mesial carina and gradually decrease in 509 size basally (Fig. 4.2, 4.3 and 4.5). The wear facet prevents from determining whether 510 there was a denticle-size discrepancy apically. Nevertheless, the distal denticles are 511 larger apically (Fig. 4.3–4.5). There is no random variation in denticle size along the 512 carinae. The denticles are almost equal in size or slightly larger on the mesial carina, 513 with a DSDI value of 1. The mesial denticle density is 15 mm per 5 mm, whereas the 514 distal denticle density is 12 denticles per 5 mm apically, 15 denticles per 5 mm at mid-515 crown, and 17 denticles per 5 mm at the base. The outline of the denticles is 516 symmetrically to slightly asymmetrically convex and perpendicular to the carinae (Fig. 517 4.1 and 4.8). The mesial denticles are mainly subquadrangular but become slightly 518 apicobasally subrectangular apically (Fig. 4.1). The distal denticles, on the other hand, 519 are mesiodistally subrectangular at mid-crown and basally, but almost subrectangular 520 apically (Fig. 4.8). Subtle interdenticular sulci are present on both carinae. These are 521 short, straight, and basally inclined.

522 A few transverse undulations are present on the crown, but they are particularly subtle. 523 Subtle marginal undulations are similarly present on the labial surface of the crown, 524 close to the distal carina. The enamel texture is non-oriented and irregular (Fig. 4.7). 525 526 **RESULTS** 527 Morphometric analyses 528 The discriminant analyses exhibit similar variance in their axes (Fig. 5 and 6). Axis 1 529 accounts for 42.45–55.62 % of the total variance, while Axis 2 explains 20.54–30.06 %. 530 The reclassification rates obtained in the LDAs are relatively high, ranging from 63.42 531 to 75.85 %, and are significantly higher using the clade-level databases (see 532 Supplementary material 1). 533 The classification of the specimens studied herein within Theropoda varies depending 534 on the database and the linear discriminant analysis (Table 1). In LDA 1 (clade level, 535 database 1), the tooth from Viso (MG 73) is classified as Abelisauridae (Jackknifed), 536 the tooth from Chera 2 (CH 168) as a non-abelisauroid ceratosaurian (Jackknifed), and 537 the Montrebei tooth (DPM-MON-T10 1) as Carcharodontosauridae (classification and 538 Jackknifed). In LDA 2 (taxon level, database 1), MG 73 is classified as Carnotaurus 539 (classification and Jackknifed), CH 168 as Gorgosaurus (Jackknifed), and DPM-MON-540 T10 1 as Acrocanthosaurus (classification and Jackknifed). In LDA 3 (clade level, 541 database 2), MG 73 is classified as a megaraptoran (Jackknifed), CH 168 as a 542 tyrannosaurid (classification and Jackknifed), and DPM-MON-T10 1 as a megaraptoran 543 (Jackknifed). In LDA 4 (taxon level, database 2), MG 73 is again classified as 544 Carnotaurus (classification and Jackknifed), CH 168 as Gorgosaurus (Jackknifed), and 545 DPM-MON-T10 1 as *Aucasaurus* (classification and Jackknifed). Finally, the 546 discriminant analysis performed using the Ibero-Armorican abelisaurid dental record

547 (Database 3) classifies MG 73 as Arcovenator (Jas Neuf Sud) (classification and 548 Jackknifed), CH 168 as the indeterminate abelisaurid teeth from Poyos, which are 549 closely related to Arcovenator (Jackknifed), and DPM-MON-T10 1 as Abelisauridae 550 indet. 1 from the Western Tremp Syncline (Jackknifed) (Table 1). 551 Cladistic analyses 552 The cladistic analysis performed on the data matrix including MG 73 and using a 553 constrained tree topology recovered a single most parsimonious tree (CI = 0.200; RI = 554 0.457; L = 1304). MG 73 is grouped with noasaurids within a well-resolved 555 Abelisauroidea clade (Fig. 7.1). The specimen from Viso shares with other 556 abelisauroids the spacing between mid-crown denticles on the distal carina, which is 557 less than one-third of the denticle width (state 0; character 107) and the presence of a 558 smooth or irregular (non-oriented) enamel-texture (state 0; character 121). The only 559 synapomorphy found for Noasauridae that can be verified in MG 73 is the average 560 number of mid-crown denticles per five millimeters on the distal carina (character 89), 561 which ranges between 16 and 29 (state 1), whereas in abelisaurids it is usually lower, 562 between 9 and 15 (state 2). Within Noasauridae, the specimen from Viso is positioned 563 as the sister taxon to Masiakasaurus, based on the presence of tenuous transverse 564 undulations on the crown (state 1; character 113). Forcing the specimen from Viso into 565 the Abelisauridae clade recovered three most parsimonious trees, with the consensus 566 tree (CI = 0.199; RI = 0.451) being four steps longer (L = 1311) than that obtained when 567 treating the specimens as floating taxon. Interestingly, constraining MG 73 within the 568 group comprising Arcovenator, Majungasaurus, and Indosuchus yielded a single most 569 parsimonious tree (CI = 0.200; RI = 0.453) and did not require additional steps (L = 570 1307) relative to the analysis with the specimens as floating taxon. However, no 571 synapomorphies were recovered for this group in the analysis.

572 The analysis performed for specimens CH 168 recovered five most parsimonious trees 573 (CI = 0.200; RI = 0.453; L = 1307) and the consensus tree (CI = 0.199; RI = 0.452; L = 0.452; L574 1309) places this specimen within Coelurosauria, allied with the tyrannosauroids 575 Gorgosaurus, Raptorex, Alioramus, Tyrannosaurus, and Daspletosaurus (Fig. 7.2). The 576 analysis found the following tyrannosauroid synapomorphies present in the Chera 2 577 specimen: (i) crown height between 1 and 6 cm (state 1; character 69); (ii) the denticles 578 on the mesial carina at two-thirds height of the crown have a subquadrangular shape 579 (state 1; character 95); and (iii) mesial and distal denticles of similar size (0.8 < DSDI < 580 1.2) (state 0; character 105). However, all these features are also shared with most 581 abelisaurids (Hendrickx et al. 2020). Forcing the specimen from Chera into the 582 Abelisauridae clade recovered three most parsimonious trees (CI = 0.199; RI = 0.451; L 583 = 1310), with the consensus tree (CI = 0.199; RI = 0.449) being five steps longer (L = 584 1314) than that obtained when treating the specimens as floating taxon. This analysis 585 recovered the following abelisaurid synapomorphies present in CH 168: (i) 586 subquadrangular shape of denticles at two-thirds height of the crown on mesial carina in 587 lateral view (state 1; character 95) and (ii) horizontal subrectangular shape of mid-588 crown denticle on distal carina in lateral view (state 1; character 96). 589 Finally, the analysis performed for DPM-MONT-T10 1 recovered seven most 590 parsimonious trees (CI = 0.200; RI = 0.454; L = 1305; consensus tree CI = 0.180; RI = 0.18591 0.376; L = 1454). The strict consensus tree shows a poor resolution, with most taxa 592 placed in a large polytomy (Fig. 8). Only a few clades such as Megalosauroidea, 593 Abelisauridae, Allosauroidea and some coelurosaurian groups are better resolved. The 594 most parsimonious trees from this analysis placed the specimen from Montrebei within 595 the Paraves clade, sometimes allied with troodontids and other times with avialan taxa. 596 Forcing the specimen into the Abelisauridae clade recovered a single most parsimonious tree (CI = 0.199; RI = 0.452) and required four additional steps (L = 1309) relative to
the most parsimonious trees obtained when treating the specimens as floating taxon. On
the other hand, constraining its position within a group comprising *Arcovenator*, *Majungasaurus*, and *Indosuchus* also yielded a single most parsimonious tree (CI =
0.199; RI = 0.451) and required only one further step (L = 1310) compared to the
previous analysis.

603

604

605

606

607

608

609

610

611

612

613

614

615

616

617

618

619

620

621

DISCUSSION

Comparisons and identification of the isolated teeth

Almost every morphometric analyses support the attribution of the MG 73 specimen to Abelisauridae, as this tooth consistently grouped within Abelisauridae, *Arcovenator*, or Carnotaurus in the LDAs (Table 1). The classification of CH 168 and DPM-MON-T10 1 is more ambiguous, as neither was grouped within Abelisauridae in any of the first three LDAs performed. Indeed, the CH 168 specimen was classified as a tyrannosaurid, a non-abelisauroid ceratosaurian, or Gorgosaurus, while DPM-MON-T10 was grouped within Carcharodontosauridae, Megaraptora, or Acrocanthosaurus. Nevertheless, DPM-MON-T10 was also grouped with Abelisauridae indet. morphotype 1 from the Western Tremp Syncline or Aucasaurus. Therefore, the morphometric analyses also strongly suggest abelisaurid affinities for this specimen. Regarding the cladistic analyses, the results do not support direct attribution of the teeth to Abelisauridae. The Viso specimen was recovered within Abelisauroidea, but more closely related to Noasauridae. Nevertheless, forcing the specimen into Abelisauridae, in a group comprising Arcovenator, Majungasaurus, and Indosuchus, does not require any additional steps, suggesting that this hypothesis is as parsimonious as the position recovered in the unconstrained analysis. The Chera 2 specimen was allied with Tyrannosauroidea.

However, all features found as synapomorphies for this clade are also shared with most abelisaurids. Forcing the specimen into Abelisauridae requires five additional steps compared to the length of the consensus tree recovered on the unconstrained analysis and one extra step to place it within the group comprising *Arcovenator*, *Majungasaurus*, and *Indosuchus*. The analysis performed for the Montrebei specimen yielded very poor resolution, with most taxa placed in a large polytomy. The most parsimonious trees placed the specimen within the Paraves clade and forcing its position into Abelisauridae required four additional steps. The lack of European abelisaurid dental and mandibular elements, along with the limited representation of European tooth data in the matrix, may account for the poor resolution of the cladistic analyses.

Abelisauridae indet.

Morphotype 1. The isolated tooth DPM-MON-T10 1 from Montrebei shares with Abelisauridae a ziphodont crown with a 'D'-shaped cross-section and the irregular, non-oriented enamel-texture (Hendrickx et al., 2019, 2020). Therefore, this tooth can be confidently assigned to Abelisauridae, which is also supported by the results of some morphometric analyses, despite the cladistic analysis not yielding sufficient resolution to test this attribution. Furthermore, the distal position of the apex and the profile of the distal margin are similar to the condition found in the distal teeth of the mesial dentition in abelisaurids, with the crown being more distally recurved (Hendrickx et al., 2020). Despite most abelisaurid taxa exhibiting a salinon-to J-shaped basal cross-section, specimen DPM-MON-T10 1 has a 'D'-shaped cross-section, as observed in Rahiolisaurus and MPCN-PV 69 (Novas et al., 2010; Gianechini et al., 2015; Hendrickx et al., 2020). The Montrebei tooth is particularly thick, a condition similarly present in the mesialmost teeth of several abelisaurid taxa such as Chenanisaurus,

647 Majungasaurus, and Rahiolisaurus (Hendrickx et al., 2020) but differing from the more 648 labiolingually compressed mesial teeth of other abelisaurids such as the premaxillary 649 teeth of Majungasaurus (see Hendrickx et al., 2020). Although the crown lacks its 650 cervical portion, it seems to have been weakly elongated, as in all known members of 651 Abelisauridae (Hendrickx et al., 2020). 652 The mesiolingually oriented mesial carina of the Montrebei specimen resembles that of 653 the first premaxillary tooth of abelisaurids, as well as some teeth possibly belonging to 654 Abelisaurus (MPCA 1, 5 and 267; see Hendrickx et al., 2020), mesial abelisaurid crowns from the Western Tremp Syncline (Abelisauridae indet. 1) and Poyos 655 656 (Abelisauridae indet. morphotype 1), along with the lateral teeth of Arcovenator and 657 closely related specimens from Poyos (Hendrickx and Mateus, 2014, Tortosa et al., 658 2014; Hendrickx et al., 2020; Isasmendi et al., 2022, 2024; Malafaia et al., 2025). The 659 strongly lingually deflected distal carina of DPM-MON-T10 is a feature shared with the mesial abelisaurid crown from the Western Tremp Syncline, the isolated mesial crown 660 661 IIPG-09, and the lateral crowns of Arcovenator (Hendrickx et al., 2020; Meso et al., 662 2021; Isasmendi et al., 2022, 2024). Two distinctive features of the Montrebei crown 663 are the position of the apex, which apparently extended beyond its basodistalmost point, 664 and its concave distal profile. These features resemble the condition seen in 'Indosuchus' and differ from the mesial dentition of Chenanisaurus, Majungasaurus, 665 666 Skorpiovenator, the mesial teeth closely related to Arcovenator from Poyos, and mesial 667 teeth from the Allen Formation in Patagonia (Smith, 2007; Hendrickx et al., 2020; Meso 668 et al., 2021; Malafaia et al., 2025). However, the distal maxillary teeth of 'Indosuchus' 669 do not exhibit a distal profile as concave as that of the Montrebei specimen (see 670 Hendrickx et al., 2020; fig. 6.f). Therefore, in light of these considerations, DPM-MON-671 T10 1 is here assigned to Abelisauridae indet.

672 Morphotype 2.

673 The isolated tooth MG 73 from Viso shares a combination of features with other members of Abelisauridae, namely a ziphodont crown, a straight or gently convex distal 674 675 profile, a lanceolate basal cross-section, denticulated mesial and distal carinae (with the 676 distal carina reaching the cervix), presence of large number of small denticles in the 677 distal carina (c. 20 denticles per 5 mm), sub-quadrangular distal denticles, narrow 678 interdenticular space, and an irregular, non-oriented enamel texture (see Hendrickx et 679 al., 2020). Furthermore, the cladistic and morphometric analyses carried out herein further support its referral to Abelisauridae or, at least to Abelisauroidea. 680 681 An irregular enamel surface texture and the presence of transverse undulations are two 682 dental features typically observed in Abelisauridae dentition (e.g., Canale et al., 2009; 683 Longrich et al., 2017; Hendrickx et al., 2019, 2020; Meso et al., 2021; Isasmendi et al., 684 2022, 2024). Transverse undulations are also present in other Iberian abelisaurid teeth 685 such as the three abelisaurid morphotypes from the latest Maastrichtian of the Western 686 Tremp Syncline (South Pyrenean Basin) (Isasmendi et al., 2024) and the teeth of 687 Arcovenator from the upper Campanian of Armuña (UPUAM 14044) and Laño (Isasmendi et al., 2022). Unlike MPZ 2004/8, MPZ 2017/804, and MPZ 2022/86 from 688 689 the Maastrichtian of Western Tremp Syncline but similar to the lateral teeth of most 690 Abelisauridae (Hendrickx et al., 2020), concave surfaces adjacent to the carinae are 691 absent in MG 73. 692 MG 73 shares a moderately compressed crown (CBR of 0.58) with Abelisaurus, 693 Arcovenator, Aucasaurus, and Majungasaurus (Hendrickx et al., 2020), as well as the 694 Abelisauridae indet. morphotypes 1 and 3 from the Western Tremp Syncline (Isasmendi 695 et al., 2024) and many teeth from Poyos (Malafaia et al., 2025).

696 Typically, the mesial and distal carinae in lateral abeliasurid crowns are centrally 697 located on their respective mesial and distal margins (Hendrickx et al., 2020). However, 698 in the MG 73 specimen, the mesial carina is lingually positioned and straight, 699 resembling the condition present in the teeth referred to Arcovenator or a closely related 700 taxon from Jas Neuf Sud, Laño, and Poyos (Tortosa et al., 2014; Hendrickx et al., 2020; 701 Isasmendi et al., 2022; Malafaia et al., 2025). The distal carina of MG 73 is centrally 702 located, as in most abelia aurids (Hendrickx et al., 2020), differing from the strongly 703 deflected distal carinae of Arcovenator from Jas Neuf Sud, the largest teeth from Laño, 704 and most of the Abelisauridae indet. lateral morphotypes from the Western Tremp 705 Syncline (Tortosa et al., 2014; Hendrickx et al. 2020; Isasmendi et al., 2022, 2024). 706 The distocentral denticle density of MG 73 is 20 denticles per five millimeters, which is 707 slightly higher than the range typically found in most Abelisauridae taxa that have 9 to 708 15 denticles per five millimeters (Hendrickx et al., 2020). The sub-quadrangular basal 709 distal denticles of MG 73 are similar in shape to those located at mid-crown in 710 Abelisaurus, Kryptops, Rugops, some Aucasaurus, and most Majungasaurus, differing 711 from the denticle shape present in Arcovenator, some teeth of Aucasaurus, and a few 712 crowns of *Majungasaurus* (Hendrickx et al., 2020). Although many abelisaurids exhibit 713 interdenticular sulci, MG 73 lacks them, similar to the condition present in the crowns 714 of Aucasaurus, Arcovenator, Rugops, and UCPC 10, which either lack these sulci or 715 have them restricted to the base of the distal denticles (Smith, 2007; Hendrickx et al., 716 2020). Therefore, despite MG 73 exhibiting many abelisaurid traits, some features are 717 distinct from any previously described member of Abelisauridae, and hence, this crown 718 is regarded as Abelisauridae indet.

719 Arcovenator sp.

720 The isolated tooth CH 168 from Chera 2 has traits present in abelisaurid teeth, including 721 an irregular and non-oriented enamel texture, CHR and CBR values, denticle shape, 722 denticle density, and the DSDI value (see Hendrickx et al., 2020). Furthermore, one of 723 the LDA classifies this specimen as *Arcovenator*. Nevertheless, the cladistic analyses do 724 not clarify the phylogenetic affinities of the Chera 2 specimen. This tooth lacks some 725 typical dental features found in most members of Abelisauridae (see Hendrickx et al., 2020), such as a straight or gently convex distal profile, a mesial carina extending to the 726 727 cervix, or the characteristic arrangement of the carinae. The CBR is moderate for a 728 lateral tooth, a feature shared with Aucasaurus, Carnotaurus, Majungasaurus, some 729 teeth assigned to Arcovenator sp. from Laño, and some teeth from Poyos (Hendrickx et 730 al., 2020; Isasmendi et al., 2022; Malafaia et al., 2025). Its CHR value is also moderate 731 (1.94), similar to those of Arcovenator, Chenanisaurus, and some lateral teeth of 732 Majungasaurus, among others (Hendrickx et al., 2020). Comparable CHR values are 733 also found in teeth assigned to Arcovenator sp. from Laño and in lateral teeth belonging 734 to an abelisaurid closely related to Arcovenator from Poyos (Isasmendi et al., 2022; 735 Malafaia et al., 2025). Furthermore, among abelisaurid teeth, only those referred to 736 Arcovenator from Armuña, Jas Neuf Sud, and Laño, as well as those closely related to 737 Arcovenator from Poyos, exhibit an apex that extends beyond the basodistalmost point 738 of the crown (Tortosa et al., 2014; Hendrickx et al., 2020; Isasmendi et al., 2022; 739 Malafaia et al., 2015; this study). 740 The lateral crowns of abelisaurid theropods typically have mesial and distal carinae that 741 extend along the midline of the crown from the apex to the root (Hendrickx et al. 2020), 742 unlike the CH 168 tooth from Chera 2. Indeed, in this specimen the mesial carina is 743 straight, displaces mesiolingually toward the base, and extends from the apex to 744 approximately two-thirds of the crown. On the other hand, the distal carina reaches the

cervix but is sigmoidal and labially deflected. This condition more closely resembles 745 746 that present in teeth referred to Arcovenator from the Jas Neuf Sud locality (Tortosa et al., 2014; Hendrickx et al., 2020), the largest teeth assigned to Arcovenator from Laño 747 748 (Isasmendi et al., 2022), and the morphotype 2 abelisaurid teeth from Poyos (Malafaia 749 et al., 2025). 750 Regarding the denticles, the DSDI value of the Chera 2 tooth is 1, similar to the teeth 751 referred to Arcovenator from Jas Neuf Sud and Laño, as well as some specimens closely 752 related to this taxon from Poyos, but differing from some Arcovenator teeth, in which 753 the DSDI exceed 1.2 (Hendrickx et al., 2020; Isasmendi et al., 2022; Malafaia et al., 754 2025). The mesiocentral denticle density of CH 168 (MC of 15 denticles per 5 mm) is 755 similar to the MC values of *Abelisaurus* and *Arcovenator*, while the distocentral denticle density of the specimen studied here (DC of 15 denticles per 5 mm) more 756 757 closely resembles those of Arcovenator or Aucasaurus, whereas Abelisaurus teeth have 758 lower DC values (Tortosa et al., 2014; Hendrickx et al., 2020). 759 The outline of the denticles in CH 168 is symmetrically to slightly asymmetrically 760 convex as in Arcovenator teeth from Jas Neuf Sud and Laño, the teeth from Poyos, 761 Skorpiovenator, and some abelisaurid teeth from the Cenomanian of northern Africa 762 (Richet et al., 2013; Hendrickx et al., 2020; Isasmendi et al., 2022; Malafaia et al., 763 2025). The CH 168 tooth further resembles the teeth of *Arcovenator* in exhibiting 764 subquadrangular or apicobasally subrectangular mesial denticles and mesiodistally 765 subrectangular distal denticles (Hendrickx et al., 2020; Isasmendi et al., 2022; Malafaia 766 et al., 2025). Therefore, based on the results of the morphometric analyses and the 767 morphological similarities of the CH 168 tooth with other Arcovenator teeth, this 768 specimen is assigned to Arcovenator sp.

769

Postcranial remains.

770

771 Despite their fragmentary nature, the Laño specimens exhibit several morphological features that support their attribution to Abelisauroidea. The presence in MCNA 17433 772 773 of a centrodiapophyseal lamina on the transverse processes of the anterior and middle 774 caudal vertebrae allows it to be confidently referred to this clade (Méndez, 2014, 775 Tortosa et al., 2014), and Abelisauridae according to Baiano et al. (2023). In addition, 776 the neural arch is also broader than the mid-centrum, which is a feature shared with 777 Masiakasaurus and several abelisaurids (Baiano et al., 2023). In addition, the elliptical 778 shape of the articular surfaces of the caudal vertebra, the presence of a ventral 779 longitudinal groove on the centrum, and the lateral orientation of transverse process of 780 the anterior dorsal and the anterior to middle caudal vertebra and the fan-shaped 781 morphology of the transverse processes of the anterior dorsal vertebra allows these 782 specimens to be referred to Majungasaurinae. Furthermore, since the presence of 783 Arcovenator has previously been documented in Laño (Isasmendi et al., 2022), these 784 remains are assigned to cf. Arcovenator sp., pending the discovery of additional 785 diagnostic material. 786 The horizontally projected transverse processes seen in MCNA 8366 are also present in 787 the anterior dorsals of *Majungasaurus* and *Sinraptor* (Currie and Zhao, 1993, 788 O'Connor, 2007) and differ from those of Allosaurus and Sigilmassasaurus (Madsen, 789 1976; Evers et al., 2015), in which the transverse processes are more ventrally 790 projected. Furthermore, the fan-shaped transverse processes, which are laterally 791 projected in MCNA 8366, are also seen in the anteriormost dorsal of *Majungasaurus* 792 and Sigilmassasaurus (O'Connor, 2007; Evers et al., 2015). The morphology of the 793 transverse process in the specimen from Laño, with an anterior convex and posterior 794 straight edge that make the diapophysis project face laterally, is similar to that of

795 Majungasaurus (UA 8678; fig. 3 of O'Connor, 2007) although in this taxon the anterior 796 convex edge is less pronounced. The posterior straight edge of the transverse processes of MCNA 8366 differs from the concave edges and posterolaterally facing diapophysis 797 798 exhibited by the anteriormost dorsals of, for instance, Carnotaurus (MACN-CH 894), 799 Eoabelisaurus (MPEF PV 3990), Viavenator (MAU-Pv-LI-530; fig. 7D of Filipi et al., 800 2018) and the indeterminate brachyrostran (MAU-Pv-LI-665; fig 6D of Méndez et al., 801 2022). This indicates that this condition could be a majungasaurine synapomorphy. 802 Nevertheless, this hypothesis needs to be phylogenetically tested. The ventral surface of the MCNA 17433 caudal vertebra exhibits a ventral longitudinal 803 804 groove, a feature also present in Allosaurus, Arcovenator, Aucasaurus, Ceratosaurus, 805 Majungasaurus, and Viavenator, as well as in many spinosaurids and megalosaurids (e.g., Madsen, 1976; Madsen and Welles, 2000; O'Connor, 2007; Benson, 2010; 806 807 Méndez, 2014; Tortosa et al., 2014; Filippi et al., 2018; Malafaia et al., 2020). This 808 contrasts with some abelisaurids, such as Ekrixinatosaurus and Rajasaurus, which 809 exhibit a keeled ventral surface (Méndez, 2014). The presence of a centrodiapophyseal 810 lamina on the ventral surface of the preserved transverse processes is a feature shared 811 with Abelisauridae (e.g., Arcovenator, Aucasaurus, Carnotaurus, Ekrixinatosaurus, 812 Kurupi and Majungasaurus) and Masiakasaurus, but not with Allosaurus or 813 Ceratosaurus (Carrano et al., 2002; Coria et al., 2002; Calvo et al., 2004; O'Connor, 814 2007; Méndez, 2014; Tortosa et al., 2014; Iori et al., 2021; Baiano et al., 2023). 815 Nevertheless, despite deformation, the bases of the transverse processes in MCNA 816 17433 do not appear to be strongly dorsally directed. This differs from many 817 abelisaurids such as Aucasaurus, Carnotaurus, Ekrixinatosaurus and Skorpiovenator, 818 and is more similar to the condition observed in Allosaurus, Arcovenator, Ceratosaurus, 819 Majungasaurus, and Rahiolisaurus (Madsen, 1976; Madsen and Welles, 2000;

820 O'Connor, 2007; Méndez, 2014; Baiano et al., 2023). The anterior and posterior 821 articular facets of the MCNA 17433 caudal vertebra are close to elliptical in outline 822 (note that although the centrum appears strongly mediolaterally compressed, this is 823 likely a taphonomic artifact). This shape is more similar to that observed in 824 Arcovenator, Majungasaurus, Rajasaurus, and Sinraptor, and differs from the more 825 subcircular surfaces of, for instance, Allosaurus, Aucasaurus, Carnotaurus, 826 Ekrixinatosaurus, Ichthyovenator, Kurupi, Tyrannosaurus or Viavenator (Currie and 827 Zhao, 1993; Brochu, 2003; Wilson et al., 2003; O'Connor, 2007; Allain et al., 2012; 828 Méndez, 2014; Tortosa et al., 2014; Filippi et al., 2018; Iori et al., 2021; Baiano et al., 829 2023). 830 New contributions to the knowledge of European abelisaurids. 831 In the Late Cretaceous European archipelago, skeletal remains of mid- to large-bodied theropods have been recovered in Central and Western Europe (e.g., Ősi et al., 2010; 832 833 Ösi and Buffetaut, 2011; Tortosa et al., 2014; Isasmendi et al., 2022; Buffetaut et al., 834 2024). Among these remains, indeterminate tetanurans and abeliaurids have been 835 identified. In the central European region, specifically at the Santonian site of Iharkút in 836 Hungary and the Campanian site of Styria in Austria, teeth assigned to early-branching indeterminate tetanurans have been recovered (Ösi et al., 2010, 2012). Additionally, the 837 838 Iharkút site has vielded further theropod remains referred to Abelisauridae (Ősi et al., 839 2010; Ösi and Buffetaut, 2011), indicating that two mid- to large-sized theropod clades 840 coexisted in Central Europe during the Santonian. However, the scarce theropod 841 remains in this area makes it challenging, at this moment, to provide a more accurate 842 interpretation of the phylogenetic relationships of this fauna. Western Europe, on the 843 other hand, appears to lack mid- to large-bodied early-branching tetanurans, with

844 Abelisauridae representing the main apex predator (e.g., Csiki-Sava et al., 2015; 845 Isasmendi et al., 2022; Buffetaut et al., 2024; Malafaia et al., 2025). Abelisaurid theropods have historically been interpreted as biogeographical indicators 846 847 of Gondwanan affinities within Late Cretaceous European dinosaur assemblages 848 (Buffetaut et al., 1988; Le Loeuff and Buffetaut, 1991; Csiki-Sava et al., 2015). Current 849 evidence supports the persistence of multiple abelisauroid lineages within the European 850 archipelago up to the latest Cretaceous (Carrano and Sampson, 2008; Tortosa et al., 851 2014; Buffetaut et al., 2024; Buffetaut, 2025). Based on the French fossil record, Tortosa et al. (2014) proposed that small-bodied abelisaurids likely originated from an 852 853 Albian lineage of early-branching abelisaurids represented by *Genusaurus sisteronis* 854 from Provence, which subsequently diversified into distinct lineages. It should be noted 855 that this taxon has, however, been variably interpreted as a noasaurid (e.g., Carrano and 856 Sampson, 2008), an early-branching abelisaurid (e.g., Tortosa et al., 2014; Baiano et al., 857 2023), or an abelisaurid more closely related to Furileusauria (Buffetaut et al., 2024; 858 Buffetaut, 2025). 859 The Cenomanian fossil record of Ibero-Armorica is scarce and currently consists of the 860 considerably incomplete Caletodraco cottardi from the early Cenomanian glauconitic 861 Chalk of Normandy (Buffetaut et al., 2024) (Fig. 9, loc. 1). This taxon, which is known 862 from ilia, some axial elements and a possible tooth, was interpreted as a furileusaurian brachyrostran, potentially reflecting a more intricate evolutionary history of European 863 864 abelisaurids, with the presence of different abelisaurid lineages in Ibero-Armorica 865 (Buffetaut, 2024; Buffetaut et al., 2024; Malafaia et al., 2025). Other Cenomanian 866 abelisaurid remains from France and Spain include isolated teeth from Algora (Segovia, 867 Spain), "La Buzinie" (Charentes, France), and Limanes (Asturias, Spain). The isolated theropod teeth from Algora (Utrillas Formation) (Fig. 9, loc. 4), were initially referred 868

869 to Carcharodontosauridae indet. (Torices et al., 2012) before being reassigned to cf. 870 Abelisauridae by Pérez-García et al. (2020). Additionally, a medium- to large-sized 871 caudal vertebra (ALG 192) from the same site was attributed to Theropoda indet. 872 (Pérez-García et al., 2020). Two other isolated teeth (MA BZN 1 and 2) from the "La 873 Buzinie" locality (Fig. 9, loc. 2) were similarly assigned to Carcharodontosauridae by 874 Vullo et al., 2007 before being reassigned to cf. Abelisauridae indet. by Malafaia et al. 875 (2025), based on their crown ornamentation and denticle densities. Another isolated 876 tooth from the Cenomanian La Manjoya Fm in the Limanes municipality (Fig. 9, loc. 3) was also identified as Theropoda indet. closely related to Carcharodontosauridae (Ruiz-877 878 Omeñaca et al., 2009). Malafaia et al. (2025) agreed on the morphometric affinities 879 suggested by Pérez-García et al. (2020) for the teeth from Algora, Charentes, and 880 Limanes. The Limanes tooth belongs to a mid-sized theropod. The apex of the crown 881 does not seem to have extended beyond its basodistalmost point (Ruiz-Omeñaca et al., 882 2009; fig. 2a and b), both mesial and distal margins are convex in lateral view (Ruiz-883 Omeñaca et al., 2009), the distal denticles are asymmetrically convex and apically 884 inclined, and the enamel exhibits an irregular texture, all features present in 885 Abelisauridae but absent in Carcharodontosauridae (Hendrickx et al., 2019, 2020). The 886 mesial carina is mesiolingually oriented (Ruiz-Omeñaca et al., 2009; fig. 2c), being 887 straight and centered apically but displaced lingually to the base, as in the first 888 premaxillary tooth of Abelisauridae, some teeth that may belong to Abelisaurus (MPCA 889 1, 5 and 267; see Hendrickx et al., 2020), Abelisauridae indet. morphotype 1 tooth from 890 the Western Tremp Syncline and Poyos, as well as in the lateral teeth of *Arcovenator* 891 and closely related specimens from Poyos (Hendrickx and Mateus, 2014, Tortosa et al., 892 2014; Hendrickx et al., 2020; Isasmendi et al., 2022, 2024; Malafaia et al., 2025). Ruiz-893 Omeñaca et al. (2009) indicate a mesial denticle density of 2 denticles/mm and a distal

894 denticle density of 2.22 denticle/mm (giving a DSDI value of 0.9). However, these 895 measurements were taken from different positions along the crown, which compromises their comparability. The inferred MA is 14 denticles per five mm and the DA is 12.5 896 897 denticles per five mm. Furthermore, an accurate DSDI value cannot be calculated 898 because the distal carina is not preserved at mid-crown. Therefore, based on the 899 combination of features shared with Abelisauridae, this tooth is here regarded as 900 Abelisauridae indet. These findings suggest that carcharodontosaurians were already 901 extinct in Ibero-Armorica by the Cenomanian and that abelisaurids had become the apex 902 theropods in those ecosystems. 903 No abelisaurid or large-sized theropod remains that may belong to Abelisauridae have 904 been recovered to date from the Turonian, Coniacian, or Santonian of the Ibero-905 Armorican landmass. In the Campanian–Maatrichtian Viso locality (Beira Litoral, 906 Portugal) (Fig. 9, loc. 5), several theropod remains were reported and figured by 907 Antunes and Sigogneau-Russell (1992) and Galton (1996). Among the Viso theropod 908 material, tooth VI 1 (Antunes and Sigogneau-Russell, 1992; pl. I, fig. 5) was initially 909 referred to as Theropoda indet. However, due to its considerable size, it may be 910 attributable to Abelisauridae as the herein studied tooth from Viso (MG 73). The MG 73 911 specimen had previously been identified as *Megalosaurus* sp. (Sauvage, 1897–1898), 912 Megalosaurus cf. pannoniensis (Lapparent and Zbyszewski, 1957), and Theropoda 913 indet. (Malafaia et al., 2024). Nonetheless, the morphological characteristics exhibited 914 by this specimen warrant its reassignment to Abelisauridae indet., representing the first 915 unequivocal abelisaurid remain from the Cretaceous of Portugal. 916 Theropod remains are relatively rare in lower Campanian deposits of Ibero-Armorica. 917 At the Lambeau du Beausset locality in Var (France) (Fig. 9, loc. 6), the abelisaurid Tarascosaurus was erected based on fragmentary material (Le Loeuff and Buffetaut, 918

919 1991). This taxon has since been regarded as nomen dubium (Rauhut, 2003; Allain and 920 Pereda-Suberbiola, 2003) or referred to Abelisauroidea incertae sedis (Carrano and 921 Sampson, 2008). Nevertheless, it was recovered as an early-branching member of 922 Abelisauridae in the phylogenetic analyses performed by Tortosa et al. (2014). 923 Additional material from the Iberian Peninsula, specifically femora from the Laño site 924 (Fig. 9, loc. 11), has been compared to *Tarascosaurus* (Le Loeuff and Buffetaut, 1991, 925 Le Loeuff, 1992), but no definitive evidence currently supports this attribution 926 (Isasmendi et al., 2021, 2022; Malafaia et al., 2025). 927 The middle and upper Campanian abelisaurid record in France and Spain is 928 comparatively richer. In Provence, indeterminate abelisaurid remains have been 929 reported from the Trets-La Boucharde site (Fig. 9, loc. 7), Velaux-Bastide Neuve (Fig. 930 9, loc. 8), and the Fox-Amphoux area (Fig. 9, loc. 9) (Tortosa et al., 2014). The Trets-La 931 Boucharde specimen from the "Begudian fluvio-lacustrine sandstones" was previously 932 described as an abelisauroid (Allain and Pereda-Suberbiola, 2003), and it is currently 933 regarded as an indeterminate abelisaurid by various authors (Carrano and Sampson, 934 2008; Tortosa et al., 2014). The abelisaurid remains reported by Tortosa et al. (2014) 935 from Velaux-Bastide Neuve ("Begudian sandstones"; Garcia et al., 2010; Cincotta et al., 936 2015) and the Fox-Amphoux area (middle—late Campanian to early Maastrichtian? 937 "Grès à reptiles") comprise a set of isolated teeth that are yet to be published. 938 Arcovenator escotae was erected based on a set of cranial, axial and appendicular 939 elements recovered from the upper Campanian Pourrières-Jas Neuf Sud locality (Fig. 9, 940 loc. 10) of the lower "Argiles rutilantes" Fm (Tortosa et al., 2014). This is the most 941 complete European abelisaurid currently known and has been classified as a 942 majungasaurine (Tortosa et al., 2014). In addition to the holotype and several referred 943 specimens reported by Tortosa et al. (2014), other skeletal elements from Upper

944 Cretaceous deposits of France and the Iberian Peninsula have also been assigned to 945 Arcovenator or closely related forms (Tortosa et al., 2014; Pérez-García et al., 2016; Isasmendi et al., 2022; Malafaia et al., 2025). This is the case of the late Campanian to 946 947 early Maastrichtian Pourcieux specimen from the Les Tuillières site ("Rognacian" 948 coarse sandstone) (Fig. 9, loc. 15) in Provence. This specimen was first regarded as 949 Abelisauridae (Buffetaut et al., 1998, Rauhut, 2003), and Abelisauridae indet. or 950 Carcharodontosauridae (Carrano and Sampson, 2008), before Tortosa et al. (2014) 951 referred it to ?Arcovenator sp. The coeval "Grès à reptiles" red beds of Cruzy in 952 Languedoc (Fig. 9, loc. 14) has yielded several teeth as well as cranial and postcranial 953 fragmentary remains, which may be attributable to medium- to large-sized abelisaurids (Buffetaut et al., 1999; Buffetaut, 2005; Ösi and Buffetaut, 2011; Tortosa et al., 2014), 954 possibly related to Arcovenator (Tortosa et al., 2014). In the Iberian Peninsula, isolated 955 956 teeth from Laño (County of Treviño), Armuña (Segovia), Chera 2 (Valencia), and 957 Poyos (Guadalajara) were assigned to Arcovenator or closely related forms (Pérez-García et al., 2016; Isasmendi et al., 2022; Malafaia et al., 2025; this work). The largest 958 959 set of isolated teeth assigned to Arcovenator sp. come from the upper Campanian 960 Sedano Fm of Laño (Fig. 9, loc. 11) (Isasmendi et al., 2022), which has also yielded 961 additional postcranial theropod remains. It must be noted that a dorsal neural arch 962 previously assigned to Rhabdodon (Pereda-Suberbiola and Sanz, 1999) and the caudal 963 vertebra herein described can be referred to cf. Arcovenator. The coeval Vegas de 964 Matute Fm of Armuña (Fig. 9, loc. 12) and Sierra Perenchiza Fm of Chera 2 (Fig. 9, loc. 965 13) have also yielded several isolated teeth referred to cf. *Arcovenator* and *Arcovenator* sp., respectively (Pérez-García et al., 2016; Company et al., 2005; this work). It is worth 966 967 noting that the isolated tooth was subject of varying taxonomic interpretations, having been referred to Theropoda indet. (Company, 2005), ?Neoceratosauria indet. (Company 968

969 et al., 2009), and cf. Arcovenator (Isasmendi et al., 2022). Additionally, the pedal 970 ungual phalanges recovered from the Armuña site were initially assigned to Theropoda indet. (Pérez-García et al., 2016) and later reinterpreted as Abelisauridae indet. 971 972 (Isasmendi et al., 2024). Two dental morphotypes from the late Campanian–early 973 Maastrichtian Poyos site (Villalba de la Sierra Fm; Gil et al., 2004; Ortega and Pérez-974 García, 2009) (Fig. 9, loc. 18) were described and referred to an abelisaurid closely 975 related to Arcovenator by Malafaia et al. (2025). This site has additionally yielded non-976 dental theropod remains initially referred to Abelisauroidea indet. (Ortega et al., 2019; 977 Pérez-García et al., 2019) and later to Abelisauridae indet. (Malafaia et al., 2025), 978 pending further detailed studies. Some theropod remain from the Lo Hueco site (Fig. 9, 979 loc. 17) were regarded as Theropoda indet. whereas others were referred to 980 Abelisauridae indet. (Ortega et al., 2015, 2022). 981 The abelisaurid fossil record from the Maastrichtian is comparatively less abundant than 982 that from the Campanian (Isasmendi et al., 2024). The early Maastrichtian Montrebei site (La Posa Formation; 'Grey Garumnian' of the Tremp Group; Fondevilla et al., 2019) 983 984 of the Tremp Syncline (Fig. 9, loc. 20) in Lleida (Iberian Peninsula) yielded an isolated 985 tooth initially assigned to Theropoda indet. (Torices et al., 2015), but its subsequent 986 restudy has permitted its referral to Abelisauridae indet. In the western section of the 987 Tremp Syncline, abelisaurid teeth were also reported from the late Maastrichtian Blasi 988 1, 2B and 3 (Fig. 9, loc. 21) and the latest Maastrichtian 172-i/04/e (Fig. 9, loc. 22) 989 sites, located at the top of the Arén Sandstone and the lower part of the Tremp Group 990 ("Grey Garumnian") (Canudo et al., 2016; Puértolas-Pascual et al., 2018; Isasmendi et 991 al., 2024). Several teeth from the Blasi sites, along with the specimen from 172-i/04/e, 992 were previously referred to Theropoda indet. by Torices et al. (2015) and Puértolas-993 Pascual et al. (2018) and later assigned to three different Abelisauridae indet.

994 morphotypes by Isasmendi et al. (2024). At the Cassagnau 1 locality (Fig. 9, loc. 16), 995 situated within the late Maastrichtian Auzas Marls Fm in Haute-Garonne, an isolated 996 tooth, originally referred to Theropoda indet. by Laurent (2003), was later reinterpreted 997 as belonging to Abelisauridae by Csiki-Sava et al. (2015). In addition to isolated teeth, 998 the Maastrichtian French deposits have yielded several indeterminate abelisaurid 999 postcranial remains. These are the limb bones (femur and tibia) initially assigned to 1000 Neoceratosauria by Valentin et al. (2012), recovered at the Vitrolles-La Plaine site (Fig. 1001 9, loc. 19) from the "Rognacian clays and mottled marls" deposits in Bouches-du-1002 Rhône. This site has been dated as possibly late Maastrichtian (Valentin et al., 2012) or 1003 also as late Campanian—early Maastrichtian (Fondevilla et al., 2019). 1004 Taken together, the abelisaurid fossil record across Ibero-Armorica reveals a complex 1005 and temporally extensive presence of this clade, spanning from the Albian to the latest 1006 Maastrichtian, with a roughly 10-million-year gap during the Turonian–Santonian 1007 without any abelisaurid fossil record. Despite their relatively fragmentary nature, these 1008 remains, ranging from isolated teeth to partial skeletons, provide compelling evidence 1009 for the persistence and diversification of abelisaurids within the European archipelago 1010 throughout the Late Cretaceous. The distribution of taxa such as Genusaurus. 1011 Caletodraco, Arcovenator, and additional indeterminate forms suggests multiple 1012 evolutionary lineages, potentially some of them stemming from an Albian stock and 1013 others likely representing subsequent dispersal events, undergoing insular 1014 diversification through the Late Cretaceous. Moreover, the taxonomic revisions of 1015 previously misassigned material emphasize the need for ongoing reevaluation of 1016 fragmentary theropod remains. Such efforts are crucial to refine our understanding of 1017 abelisaurid paleobiogeography and systematics in Europe.

1018

CONCLUSIONS

1019

1020 The systematic, morphometric and cladistic studies carried out with the tooth sample 1021 from late Campanian Chera 2 (Valencia), early Maastrichtian Montrebei (Lleida) and 1022 Campanian–Maastrichtian Viso (Beira Litoral) localities from the Iberian Peninsula 1023 have allowed to reassign these elements to abelisaurids. Although incomplete, the 1024 Montrebei (DPM-MON-T10 1) and Viso (MG 73) specimens differ from the dentition 1025 of the already erected members of Abelisauridae. On the other hand, the crown-shape, 1026 disposition of the carinae and denticle shape exhibited by CH 168 tooth from Chera 2 1027 are similar to those found in Arcovenator teeth. Hence, the Montrebei and Viso teeth are 1028 now considered to belong to Abelisauridae indet., while the Chera 2 specimen is 1029 attributed to Arcovenator sp. In addition, the postcranial remains (axial elements) 1030 recovered from the Laño site (County of Treviño) are here regarded to as an abelisaurid, 1031 mainly based on the presence of a centrodiapophyseal lamina on the preserved 1032 transverse process in the caudal vertebra (MCNA 17433). In addition, the shape and 1033 orientation of the transverse processes of the dorsal and caudal vertebrae suggest 1034 majungasaurine affinities. Therefore, these features, together with the presence of 1035 Arcovenator teeth in the site, allow us to assign these elements to cf. Arcovenator. The 1036 revision of the Laño postcranial remains has allowed to refute earlier interpretations that 1037 assigned the anterior dorsal neural arch (MCNA 8366) to Rhabdodon. Furthermore, the 1038 Viso isolated tooth, now assigned to Abelisauridae indet., is the first unequivocal 1039 abelisaurid remain from Portugal. 1040 The fossil record indicates that abelisaurids were among the most prevalent theropod 1041 groups in the Late Cretaceous faunas across the Ibero-Armorican landmasses. Indeed, 1042 the reclassification of mid- to large-sized isolated teeth from Ibero-Armorica as 1043 belonging to abelisaurids, rather than to carcharodontosaurids or closely related forms,

1044 indicates that carcharodontosaurians were likely extinct in Ibero-Armorica by the 1045 Cenomanian, and that abelisaurids had already taken over as the dominant large 1046 theropods in those ecosystems. 1047 The abelisaurid fossil record from Ibero-Armorica reveals a complex and temporally 1048 extensive presence of this clade, spanning from the Albian to the latest Maastrichtian, 1049 with a significant gap of approximately 10 million years during the Turonian— 1050 Santonian, in which no abelisaurid fossils have been found yet. Despite the generally 1051 fragmentary nature of these remains, ranging from isolated teeth to partial skeletons, 1052 they provide strong evidence for the persistence and diversification of abelisaurids 1053 across the European archipelago. The distribution of taxa such as the noasaurid or 1054 possibly furileusaurian Genusaurus, the putative furileusaurian Caletodraco, the 1055 majungasaurine Arcovenator, and other indeterminate forms suggests the presence of 1056 multiple evolutionary lineages, some potentially originating from an Albian stock, while 1057 others might have resulted from several dispersal events, undergoing insular 1058 diversification throughout the Late Cretaceous. Additionally, the taxonomic revisions of 1059 previously misclassified material underscore the need to continuously reevaluate 1060 fragmentary theropod remains, thereby refining our understanding of abelisaurid 1061 paleobiogeography and systematics in Europe.

1062

1063

1064

1065

1066

1067

1068

ACKNOWLEDGMENTS

We would like to thank Xabier Pereda-Suberiola (UPV/EHU), Angélica Torices (UCM), Carmelo Corral (MCNA), Concha Herrero (UCM), Jorge Sequeira and Rúben Dias (MG) for granting us access to the herein studied material. We are also thankful to Julio Company (UPV) for sharing the photographs of the Chera 2 specimen. Special thanks are due to Elena Cuesta (SNSB-BSPG), Manuel Pérez-Pueyo (UPV/EHU) and

1069 Ignacio Díaz-Martinez (UC) for their helpful advice. We also thank Mattia Baiano 1070 (UNRN) for sharing the photographs of the South American abeliaaurids. Finally, we 1071 would also like to thank Taylor Swift and Lady Gaga for making the writing of this 1072 manuscript more enjoyable. This work was supported by the Spanish Ministry of 1073 Science, Innovation and Universities and the European Regional Development Fund 1074 (projects CGL2017-85038-P and PID2021-122612OBI00, MINECO/FEDER, UE), the 1075 Basque Government/Eusko Jaurlaritza (research groups IT418-19 and IT1485-22), and 1076 the Portuguese Fundação para a Ciência e a Tecnologia (FCT) I.P./MCTES through and 1077 individual contracts CEECIND/01770/2018 1078 (https://doi.org/10.54499/CEECIND/01770/2018/CP1534/CT0004). We are very 1079 thankful to Scott Hartman for letting us use his skeletal diagrams and Willi Henning 1080 Society for the available free TNT software. We especially thank the editors Mauricio 1081 Cerroni and Diego Pol, and the referees Matias Soto and Christophe Hendrickx for their 1082 comments and suggestions that greatly improved the manuscript. 1083 1084 **REFERENCES** 1085 Allain, R., & Taquet, P. (2000). A new genus of Dromaeosauridae (Dinosauria, 1086 Theropoda) from the Upper Cretaceous of France. *Journal of Vertebrate* 1087 Paleontology, 20(2), 404–407. https://doi.org/10.1671/0272-1088 4634(2000)020[0404:ANGODD]2.0.CO;2 1089 Allain, R., & Pereda-Suberbiola, X. (2003). Dinosaurs of France. Comptes Rendus 1090 Palevol, 2(1), 27–44. https://doi.org/10.1016/S1631-0683(03)00002-2 1091 Allain, R., Xaisanavong, T., Richir, P., & Khentavong, B. (2012). The first definitive 1092 Asian spinosaurid (Dinosauria: Theropoda) from the early cretaceous of Laos. 1093 *Naturwissenschaften*, 99(5), 369–377. https://doi.org/10.1007/s00114-012-0911-7

- 1094 Alonso, A., Meléndez, N., & Mas, J. R. (1991). Sedimentación lacustre durante el 1095 Cretácico en la Cordillera Ibérica, España. Acta geológica hispánica, 26, 35–54. 1096 Amudeo-Plaza, J., Soto-Acuna, S., Ugalde, R., Martínez, P., & Rubilar-Rogers, D. 1097 (2023). Reassessment of theropod material from Pichasca, Northern Chile: 1098 Presence of Abelisauridae (Theropoda: Ceratosauria) from the Quebrada La 1099 Totora Beds (Albian-Turonian). Journal of South American Earth Sciences, 129, 1100 104494. https://doi.org/10.1016/j.jsames.2023.104494 1101 Antunes, M. T., & Sigogneau-Russell, D. (1991). Nouvelles données sur les dinosaures 1102 du Crétacé supérieur du Portugal. Comptes Rendus de l'Académie des Sciences, 1103 Paris, II, 313, 113–119. 1104 Antunes, M. T., & Sigogneau-Russell, D. (1992). La faune de petits dinosaures du
- Antunes, M. T., & Sigogneau-Russell, D. (1992). La faune de petits dinosaures du
 Crétacé terminal portugais. Comunicações dos Serviços Geológicos de Portugal,
 78(1), 49–62.
- 1107 Ardèvol, L., Klimowitz, J., Malagón, J., & Nagtegaal, P. J. C. (2000). Depositional
 1108 Sequence Response to Foreland Deformation in the Upper Cretaceous of the
 1109 Southern Pyrenees, Spain. *AAPG Bulletin*, 84(4), 566–587.
- 1110 https://doi.org/10.1306/C9EBCE55-1735-11D7-8645000102C1865D
- 1111 Astibia, H., Buffetaut, E., Buscalioni, A. D., Cappetta, H., Corral, C., Estes, R., García-1112 Garmilla, F., Jaeger, J. J., Jiménez-Fuentes, E., Le Loeuff, J., Mazin, J. M., Orue-
- Etxebarria, X., Pereda-Suberbiola, J., Powell, J. E., Rage, J. C., Rodriguez-
- 1114 Lázaro, J., Sanz, J. L., & Tong, H. (1990). The fossil vertebrates from Laño
- 1115 (Basque Country, Spain); new evidence on the composition and affinities of the
- Late Cretaceous continental faunas of Europe. *Terra Nova*, 2(5), 460–466.
- 1117 Astibia, H., Murelaga, X., Pereda-Suberbiola, X., Elorza, J. J., & Gómez-Alday, J. J.
- 1118 (1999). Taphonomy and palaeoecology of the Upper Cretaceous continental

1119	vertebrate-bearing beds of the Laño quarry (Iberian Peninsula). Estudios del
1120	Museo de Ciencias naturales de Alava, 14(Número especial 1), 43-104.
1121	Baiano, M. A., Coria, R. A., Canale, J. I., & Gianechini, F. A. (2021). New abelisaurid
1122	material from the Anacleto Formation (Campanian, Upper Cretaceous) of
1123	Patagonia, Argentina, shed light on the diagnosis of the Abelisauridae
1124	(Theropoda, Ceratosauria). Journal of South American Earth Sciences, 110,
1125	103402. https://doi.org/10.1016/j.jsames.2021.103402
1126	Baiano, M. A., Coria, R., Chiappe, L. M., Zurriaguz, V., & Coria, L. (2023). Osteology
1127	of the axial skeleton of Aucasaurus garridoi: phylogenetic and paleobiological
1128	inferences. <i>PeerJ</i> , 11, e16236. https://doi.org/10.7717/peerj.16236
1129	Barbosa, B. P., Soares, A. F., Rocha, R. B., Manuppella, G., & Henriques, M. H.
1130	(2008). Geological map of Portugal at a scale of 1:50.000: explanatory news of
1131	the sheet 19-A (Cantanhede). Departamento de Geologia, Instituto Nacional de
1132	Engenharia, Tecnologia e Inovação, Lisboa.
1133	Benson, R. B. (2010). A description of Megalosaurus bucklandii (Dinosauria:
1134	Theropoda) from the Bathonian of the UK and the relationships of Middle
1135	Jurassic theropods. Zoological Journal of the Linnean Society, 158, 882–935.
1136	https://doi.org/10.1111/j.1096-3642.2009.00569.x
1137	Berreteaga, A. (2008). Estudio estratigráfico, sedimentológico y paleontológico de los
1138	yacimientos con fósiles de vertebrados del Cretácico final de la Región Vasco-
1139	Cantábrica (Tesis Doctoral, Facultad de Ciencia y Tecnología, Universidad del
1140	País Vasco, Leioa).
1141	Bonaparte, J. F. (1991). The gondwanian theropod families Abelisauridae and
1142	Noasauridae. Historical Biology, 5(1), 1–25.
1143	https://doi.org/10.1080/10292389109380385

- Bonaparte, J. F. (1996). Cretaceous tetrapods of Argentina. Münchner
- 1145 *Geowissenschaftliche Abhandlungen*, 30(7), 73–130.
- Bonaparte, J. F., & Novas, F. E. (1985). Abelisaurus comahuensis n. g., n. sp.,
- 1147 Carnosauria del Cretacico tardia de Patagonia. *Ameghiniana*, 22, 259–265.
- Brochu, C. A. (2003). Osteology of *Tyrannosaurus rex*: insights from a nearly complete
- skeleton and high-resolution computed tomographic analysis of the skull. *Journal*
- of Vertebrate Paleontology, 22(4 suppl.), 1–138.
- 1151 https://doi.org/10.1080/02724634.2003.10010947
- Buffetaut, E. (2005). Late Cretaceous vertebrates from the Saint-Chinian area (southern
- France): a review of previous research and an update on recent finds. *Acta*
- 1154 Palaeontologica Romaniae, 5(3), 39–48.
- Buffetaut, E. (2024). The discontinuous fossil record of European Abelisauridae and its
- significance for abelisaurid evolution and palaeobiogeography. *Evolução*, 3, 19–
- 1157 21.
- Buffetaut, E. (2025). Furileusaurian osteological characters in *Genusaurus sisteronis*
- 1159 Accarie et al., 1995, an abelisaurid dinosaur from the Albian (Lower Cretaceous)
- of south-eastern France. *Carnets natures*, 12, 79–88.
- Buffetaut, E., Mechin, P., & Mechin-Salessy, A. (1988). Un dinosaure théropode
- d'affinités gondwaniennes dans le Crétacé supérieur de Provence. *Comptes*
- 1163 Rendus de l'Académie des Sciences II, 306, 153–158.
- Buffetaut, E., Le Leuff, J., Tong, H., Duffaud, S., Cavin, L., Garcia, G., & Ward, D.
- 1165 (1999). Un nouveau gisement de vertébrés du Crétacé supérieur à Cruzy (Hérault,
- Sud de la France). *Comptes Rendus de l'Académie des Sciences II*, 328, 203–208.
- 1167 https://doi.org/10.1016/S1251-8050(99)80097-4

1168 Buffetaut, E., Tong, H., Girard, J., Hoyez, B., & Párraga, J. (2024). Caletodraco 1169 cottardi: A New Furileusaurian Abelisaurid (Dinosauria: Theropoda) from the 1170 Cenomanian Chalk of Normandy (North-Western France). Fossil Studies, 2(3), 1171 177–195. https://doi.org/10.3390/fossils2030009 1172 Calvo, J. O., Rubilar-Rogers, D., & Moreno, K. (2004). A new abelisauridae 1173 (Dinosauria: Theropoda) from northwest Patagonia. Ameghiniana, 41(4), 555– 1174 563. 1175 Canale, J. I., Scanferla, C. A., Agnolin, F. L., & Novas, F. E. (2009). New carnivorous 1176 dinosaur from the Late Cretaceous of NW Patagonia and the evolution of 1177 abelisaurid theropods. Naturwissenschaften, 96, 409–414. 1178 https://doi.org/10.1007/s00114-008-0487-4 1179 Candeiro, C. R. A., & Martinelli, A. G. (2005). Abelisauroidea and 1180 Carchardontosauridae (Theropoda, Dinosauria) in the Cretaceous of South 1181 America. Paleogeographical and geocronological implications. Sociedade & 1182 Natureza, Uberlândia, 17, 5–19. 1183 Canudo, J. I., Oms, O., Vila, B., Galobart, A., Fondevilla, V., Puértolas-Pascual, E., 1184 Sellés, A. G., Cruzado-Caballero, P., Dinarès-Turell, J., Vicens, E., Castanera, D., 1185 Company, J., Burrel, L., Estrada, R., Marmi, J., & Blanco, A. (2016). The upper 1186 Maastrichtian dinosaur fossil record from the southern Pyrenees and its 1187 contribution to the topic of the Cretaceous-Palaeogene mass extinction event. 1188 Cretaceous Research, 57, 540–551. https://doi.org/10.1016/j.cretres.2015.06.013 1189 Carrano, M. T., & Sampson, S. D. (2008). The phylogeny of ceratosauria (Dinosauria: 1190 Theropoda). *Journal of Systematic Palaeontology*, 6(2), 183–236.

https://doi.org/10.1017/S1477201907002246

1191

1192 Carrano, M. T., Sampson, S. D., & Forster, C. A. (2002). The osteology of 1193 Masiakasaurus knopfleri, a small abelisauroid (Dinosauria: Theropoda) from the 1194 Late Cretaceous of Madagascar. Journal of Vertebrate Paleontology, 22(3), 510-1195 534. https://doi.org/10.1671/0272-4634(2002)022[0510:TOOMKA]2.0.CO;2 1196 Carrano, M. T., Benson, R. B., & Sampson, S. D. (2012). The phylogeny of tetanurae 1197 (Dinosauria: Theropoda). Journal of Systematic Palaeontology, 10(2), 211–300. 1198 https://doi.org/10.1080/14772019.2011.630927 1199 Cerroni, M. A., Canale, J. I., Novas, F. E., & Paulina-Carabajal, A. (2022). An 1200 exceptional neurovascular system in abelisaurid theropod skull: new evidence 1201 from Skorpiovenator bustingorryi. Journal of Anatomy, 240(4), 612–626. 1202 https://doi.org/10.1111/joa.13258 1203 Cincotta, A., Yans, Y., Godefroit, P., Garcia, G., Dejax, J., Benammi, M., Amico, S., & 1204 Valentin, X. (2015). Interated paleoenvironmental reconstruction and taphonomy 1205 of a unique Upper Cretaceous vertebrate-bearing locality (Velaux, southeastern 1206 France). *PLOS ONE*, 10(8), e0134231. 1207 https://doi.org/10.1371/journal.pone.0134231 1208 Company, J. (2005). Vertebrados continentales del Cretácico superior (Campaniense-1209 Maastrichtiense) de Valencia (Tesis Doctoral, Facultad de Ciencias Biológicas, 1210 Universitat de València, Valencia). 1211 Company, J., & Szentesi, Z. (2012). Amphibians from the Late Cretaceous Sierra 1212 Perenchiza Formation of the Chera Basin, Valencia Province, Spain. Cretaceous 1213 Research, 37, 240–245. https://doi.org/10.1016/j.cretres.2012.04.003 1214 Company, J., Feist, M., Peyrot, D., Barrón, E., Robles, F., Pereda-Suberbiola, X., & 1215 Ruiz-Omeñaca, J. I. (2005). Stratigraphic position and palaeoenvironmental traits

1216 of the Late Cretaceous vertebrate-bearing sites of Chera (Valencia, Spain), based 1217 on micropalaeontological data. Kaupia, 14, 76. 1218 Company, J., Torices, A., Pereda-Suberbiola, X., & Ruiz-Omeñaca, J. (2009). Theropod 1219 teeth from the Late Cretaceous of Chera (Valencia, eastern Spain). Journal of 1220 Vertebrate Paleontology, 29, 81A. 1221 Coria, R. A., Chiappe, L. M., & Dingus, L. (2002). A new close relative of *Carnotaurus* 1222 sastrei Bonaparte 1985 (Theropoda: Abelisauridae) from the Late Cretaceous of 1223 Patagonia. Journal of Vertebrate Paleontology, 22(2), 460–465. 1224 https://doi.org/10.1671/0272-4634(2002)022[0460:ANCROC]2.0.CO;2 1225 Corral, J. C., Pueyo, E. L., Berreteaga, A., Rodríguez-Pintó, A., Sánchez, E., & Pereda-1226 Suberbiola, X. (2016). Magnetostratigraphy and lithostratigraphy of the Laño 1227 vertebrate-site: Implications in the uppermost Cretaceous chronostratigraphy of the Basque-Cantabrian Region. Cretaceous Research, 57, 473–489. 1228 1229 https://doi.org/10.1016/j.cretres.2015.07.015 1230 Csiki-Sava, Z., Buffetaut, E., Ösi, A., Pereda-Suberbiola, X., & Brusatte, S. L. (2015). 1231 Island life in the Cretaceous-faunal composition, biogeography, evolution, and 1232 extinction of land-living vertebrates on the Late Cretaceous European archipelago. 1233 ZooKeys, 469, 1–161. https://doi.org/10.3897/zookeys.469.8439 1234 Currie, P. J., & Zhao, X. J. (1993). A new carnosaur (Dinosauria, Theropoda) from the 1235 Jurassic of Xinjiang, People's Republic of China. Canadian Journal of Earth 1236 Sciences, 30(10), 2037–2081. https://doi.org/10.1139/e93-179 1237 Currie, P. J., Rigby Jr., J. K., & Sloan, R. E. (1990). Theropod teeth from the Judith 1238 River Formation of southern Alberta, Canada. In K. Carpenter, & P. J. Currie, 1239 (Eds.). *Dinosaur Systematics: perspectives and approaches* 8 (pp. 107–125). 1240 Cambridge University Press.

1241 Díez-Canseco, D., Arz, J. A., Benito, M. I., Díaz-Molina, M., & Arenillas, I. (2014). 1242 Tidal influence in redbeds: A palaeoenvironmental and biochronostratigraphic 1243 reconstruction of the Lower Tremp Formation (South-Central Pyrenees, Spain) 1244 around the Cretaceous/Paleogene boundary. Sedimentary Geology, 312, 31–49. 1245 https://doi.org/10.1016/j.sedgeo.2014.06.008 1246 Eichenseer, H. (1988). Facies Geology of Late Maastrichtian to Early Eocene Coastal 1247 and Shallow Marine Sediments (Tremp-Graus Basin, Northeastern Spain) (Tesis 1248 Doctoral, Institut und Museum für Geologie und Paläontologie, Universität 1249 Tübingen, Tübingen). 1250 Evers, S. W., Rauhut, O. W. M., Milner, A. C., McFeeters, B., & Allain, R. (2015). A 1251 reappraisal of the morphology and systematic position of the theropod dinosaur 1252 Sigilmassasaurus from the "middle" Cretaceous of Morocco. PeerJ, 3, e1323. 1253 https://doi.org/10.7717/peerj.1323 1254 Filippi, L. S., Méndez, A. H., Gianechini, F. A., Valieri, R. D. J., & Garrido, A. C. 1255 (2018). Osteology of Viavenator exxoni (Abelisauridae; Furileusauria) from the 1256 Bajo de la Carpa Formation, NW Patagonia, Argentina. Cretaceous Research, 83, 1257 95–119. https://doi.org/10.1016/j.cretres.2017.07.019 1258 Floquet, M., Alonso, A., & Melendez, A. (1982). Cameros-Castilla. El Cretácico 1259 Superior. In A. García (Ed.). *El Cretácico de España*. Editorial Complutense. 1260 Fondevilla, V., Dinarès-Turell, J., & Oms, O. (2016). The chronostratigraphic 1261 framework of the South-Pyrenean Maastrichtian succession reappraised: 1262 Implications for basin development and end Cretaceous dinosaur faunal turnover. 1263 Sedimentary Geology, 337, 55–68. https://doi.org/10.1016/j.sedgeo.2016.03.006 1264 Fondevilla, V., Riera, V., Vila, B., Dinarès-Turell, J., Vicens, E., Gaete, R., Oms, O., & 1265 Galobart, À. (2019). Chronostratigraphic synthesis of the latest Cretaceous

- dinosaur turnover in south-western Europe. *Earth-Science Reviews*, 191, 168–189.
- 1267 https://doi.org/10.1016/j.earscirev.2019.01.007
- Galton, P. M. (1996). Notes on Dinosauria from the Upper Cretaceous of Portugal.
- 1269 Neues Jahrbuch für Geologie und Paläontologie Monatshefte, 2, 83–90.
- 1270 Garcia, G., Duffaud, S., Feist, M., Marandat, B., Tambareau, Y., Villatte, J., & Sigé, B.
- 1271 (2000). La Neuve, gisement à plantes, invertébrés et vertébrés du Bégudien
- 1272 (Sénonien supérieur continental) du bassin d'Aix-en-Provence. *Geodiversitas*,
- 1273 22(3), 325–348.
- 1274 Garcia, G., Amico, S., Fournier, F., Thouand, E., & Valentin, X. (2010). A new
- titanosaur genus (Dinosauria, Sauropoda) from the Late Cretaceous of southern
- France and its paleobiogeographic implications. Bulletin de la Société Géologique
- de France, 181, 269–277. https://doi.org/10.2113/gssgfbull.181.3.269
- 1278 Gianechini, F. A., Apesteguía, S., Landini, W., Finotti, F., Valieri, R. J., & Zandonai, F.
- 1279 (2015). New abelisaurid remains from the Anacleto Formation (Upper
- 1280 Cretaceous), Patagonia, Argentina. *Cretaceous Research*, 54, 1–16.
- 1281 https://doi.org/10.1016/j.cretres.2014.11.009
- 1282 Gil, J., Carenas, B., Segura, M., García-Hidalgo, J. F., & García, A. (2004). Revisión y
- correlación de las unidades listoestratigráficas del Cretácico Superior de la región
- central y oriental de España. Revista de la Sociedad Geológica de España, 17,
- 1285 249–266.
- 1286 Goloboff, P. A., & Morales, M. E. (2023). TNT version 1.6, with a graphical interface
- for MacOS and Linux, including new routines in parallel. *Cladistics*, *39*, 144–153.
- 1288 https://doi.org/10.1111/cla.12524.
- 1289 Gómez, J. J., Sandoval, J., Aguado, R., O'Dogerthy, L., & Osete, M. L. (2019). The
- 1290 Alpine Cycle in Eastern Iberia: Microplate Units and Geodynamic Stages. In C.

1291 Quesada, & J. T. Oliveira (Eds.). The Geology of Iberia: A Geodynamic 1292 Approach, volume 3: The Alpine Cycle. Regional Geology Reviews (pp. 15–28). 1293 Springer. Gómez-Alday, J. J. (1999). Stratigraphy and depositional environments of the Upper 1294 1295 Cretaceous of the Laño quarry. Evidence of diapiric activity. Estudios del Museo de Ciencias Naturales de Álava, 14(Número especial 1), 29–35. 1296 1297 Hammer, Ø., Harper, D. A. T., & Ryan, P. D. (2001). PAST: paleontological statistics 1298 software package for education and data analysis. Palaeontologia Electronica, 1299 *4*(1), 1–9. 1300 Hendrickx, C., & Mateus, O. (2014). Abelisauridae (Dinosauria: Theropoda) from the 1301 Late Jurassic of Portugal and dentition-based phylogeny as a contribution for the 1302 identification of isolated theropod teeth. Zootaxa, 3759, 1–74. 1303 Hendrickx, C., Hartman, S. A., & Mateus, O. (2015a). An overview of non-avian 1304 theropod discoveries and classification. PalArch's Journal of Vertebrate 1305 *Palaeontology*, *12*(1), 1–73. 1306 Hendrickx, C., Mateus, O., & Araújo, R. (2015b). A proposed terminology of theropod 1307 teeth (Dinosauria, Saurischia). Journal of Vertebrate Paleontology, 35, e982797. 1308 https://doi.org/10.1080/02724634.2015.982797 1309 Hendrickx, C., Mateus, O., Araújo, R., & Choiniere, J. (2019). The distribution of 1310 dental features in non-avian theropod dinosaurs: Taxonomic potential, degree of homoplasy, and major evolutionary trends. Palaeontologia Electronica, 22(3), 74. 1311 1312 https://doi.org/10.26879/820 1313 Hendrickx, C., Tschopp, E., & d. Ezcurra, M. (2020). Taxonomic identification of 1314 isolated theropod teeth: the case of the shed tooth crown associated with

1315 Aerosteon (Theropoda: Megaraptora) and the dentition of Abelisauridae. 1316 Cretaceous Research, 108, 104312. https://doi.org/10.1016/j.cretres.2019.104312 1317 Iori, F. V., Araújo-Júnior, H. I. de, Tavares, S. A. S., Silva Marinho, T. da, & Martinelli, 1318 A. G. (2021). New theropod dinosaur from the Late Cretaceous of Brazil 1319 improves abelisaurid diversity. Journal of South American Earth Sciences, 112, 1320 103551. https://doi.org/10.1016/j.jsames.2021.103551 1321 Isasmendi, E., Torices, A., Canudo, J. I., & Pereda-Suberbiola, X. (2021). Abelisaurid 1322 dinosaurs from the Upper Cretaceous Laño site (Iberian Peninsula). Ciências da 1323 *Terra Procedia*, 1, 38–41. https://doi.org/10.21695/cterraproc.v1i0.401 1324 Isasmendi, E., Torices, A., Canudo, J. I., Currie, P. J., & Pereda-Suberbiola, X. (2022). 1325 Upper Cretaceous European theropod palaeobiodiversity, palaeobiogeography and 1326 the intra-Maastrichtian faunal turnover: new contributions from the Iberian fossil 1327 site of Laño. *Papers in Palaeontology*, 8(1), e1419. 1328 https://doi.org/10.1002/spp2.1419 Isasmendi, E., Pérez-Pueyo, M., Moreno-Azanza, M., Alonso, A., Puértolas-Pascual, E., 1329 1330 Bádenas, B., & Canudo, J. I. (2024). Theropod teeth palaeodiversity from the 1331 uppermost Cretaceous of the South Pyrenean Basin (NE Iberia) and the intra-1332 Maastrichtian faunal turnover. Cretaceous Research, 162, 105952. 1333 https://doi.org/10.1016/j.cretres.2024.105952 1334 Lapparent, A. F., & Zbyszewski, G. (1957). The dinosaurs from Portugal. *Memoire* 1335 Services Géologiques du Portugal, 2(nouvelle série), 1–131. 1336 Laurent, Y. (2003). Les faunes de vertébrés continentaux du Maastrichtien supérieur 1337 d'Europe: systématique et biodiversité. Strata, série 2, 41, 1–81.

- Laurent, Y., Bilotte, M., & Le Loeuff, J. (2002). Late Maastrichtian continental
- vertebrates from southwestern France: correlation with marine fauna.
- 1340 Palaeogeography, Palaeoclimatology, Palaeoecology, 187(1–2), 121–135.
- 1341 Lavocat, R. (1955). Sur une portion de mandibule de Théropode provenant du Crétacé
- supérieur de Madagascar. Bulletin du Muséum National d'Histoire Naturelle de
- 1343 *Paris*, 27(2), 256–259.
- Le Loeuff, J., & Buffetaut, E. (1991). *Tarascosaurus salluvicus* nov. gen., nov. sp.,
- dinosaure théropode du Crétacé supérieur du Sud de la France. *Geobios*, 24(5),
- 1346 585–594.
- 1347 Le Loeuff, J. (1992). Les vertébrés continentaux du Crétacé supérieur d'Europe:
- paléoécologie, biostratigraphie et paléobiogéographie (Tesis Doctoral, Université
- 1349 Pierre & Marie Curie, Paris, Paris).
- Longrich, N. R., Pereda-Suberbiola, X., Jalil, N. E., Khaldoune, F., & Jourani, E.
- 1351 (2017). An abelisaurid from the latest Cretaceous (late Maastrichtian) of Morocco,
- North Africa. Cretaceous Research, 76, 40–52.
- https://doi.org/10.1016/j.cretres.2017.03.021
- 1354 Maddison, W. P., & Maddison, D. R. (2011). Mesquite: a modular system for
- 1355 evolutionary analysis. Retrieved May 23, 2012, from http://mesquiteproject.org.
- 1356 Madsen, J. H. Jr (1976). Allosaurus fragilis: a revised osteology. Utah Geological
- 1357 Survey Bulletin, 109, 1–163.
- 1358 Madsen, J. H. Jr, & Welles, S. P. (2000). Ceratosaurus (Dinosauria, Theropoda), a
- revised osteology. *Utah Geological Survey, Miscellaneous Publication*, 2, 1–80.
- Malafaia, E., Mocho, P., Escaso, F. & Ortega, F. (2020). A new carcharodontosaurian
- theropod from the Lusitanian Basin: evidence of allosauroid sympatry in the

- European Late Jurassic. *Journal of Vertebrate Paleontology*, 40(1), e1768106.
- 1363 https://doi.org/10.1080/02724634.2020.1768106
- Malafaia, E., Escaso, F., Coria, R. A., & Ortega, F. (2023). An Eudromaeosaurian
- 1365 Theropod from Lo Hueco (Upper Cretaceous. Central Spain). *Diversity*, 15(2),
- 1366 141. https://doi.org/10.3390/d15020141
- Malafaia, E., Mocho, P., Escaso, F., Narvaéz, I., & Ortega, F. (2024). Taxonomic and
- stratigraphic update of the material historically attributed to *Megalosaurus* from
- 1369 Portugal. *Palaeontologia Polonica*, 69(2), 127–171.
- 1370 https://doi.org/10.4202/app.01113.2023
- Malafaia, E., Escaso, F., Coria, R. A., Pérez-García, A., & Ortega, F. (2025). Theropod
- teeth from the Upper Cretaceous of central Spain: Assessing the
- paleobiogeographic history of European abelisaurids. Cretaceous Research, 168,
- 1374 106072. https://doi.org/10.1016/j.cretres.2024.106072
- 1375 Marmi, J., Blanco, A., Fondevilla, V., Dalla Vecchia, F. M., Sellés, A. G., Vicente, A.,
- Martín-Closas, C., Oms, O., & Galobart, A. (2016). The Molí del Baró-1 site, a
- diverse fossil assemblage from the uppermost Maastrichtian of the southern
- 1378 Pyrenees (north-eastern Iberia). *Cretaceous Research*, *57*, 519–539.
- 1379 https://doi.org/10.1016/j.cretres.2015.06.016
- 1380 Marsh, O. C. (1881). Principal characters of American Jurassic dinosaurs. Part V.
- 1381 American Journal of Science, 21(Series 3), 417–423.
- 1382 Marsh, O. C. (1884). Principal characters of the American Jurassic dinosaurs. Part VIII.
- The order Theropoda. *American Journal of Science*, 27, 329–340.
- Martín-Chivelet, J., Floquet, M., García-Senz, J., Callapez, P. M., Lopez-Mir, B.,
- Muñoz, J. A., Barroso-Barcenilla, F., Segura, M., Ferreira Soares, A., Morgado
- Dinis, P., Fonseca Marques, J., & Arbues, P. (2019). Late Cretaceous post-rift to

1387 convergence in Iberia. In C. Quesada, & J. T. Oliveira (Eds.). The geology of 1388 Iberia: A geodynamic approach, Vol. 3, The Alpine Cycle. Springer. 1389 Méndez, A. H. (2014). The caudal vertebral series in abelisaurid dinosaurs. Acta 1390 Palaeontologica Polonica, 59(1), 99–107. https://doi.org/10.4202/app.2012.0095 1391 Méndez, A. H., Gianechini, F. A., Paulina-Carabajal, A., Filippi, L. S., Juárez-Valieri, 1392 R. D., Cerda, I. A., & Garrido, A. C. (2022). New furileusaurian remains from La 1393 Invernada (northern Patagonia, Argentina): A site of unusual abelisaurids 1394 abundance. Cretaceous Research, 129, 104989. 1395 https://doi.org/10.1016/j.cretres.2021.10498 1396 Meso, J. G., Hendrickx, C., Baiano, M. A., Canale, J. I., Salgado, L., & Díaz Martínez, 1397 I. (2021). Isolated theropod teeth associated with a sauropod skeleton from the 1398 Late Cretaceous Allen Formation of Río Negro, Patagonia, Argentina. Acta 1399 *Palaeontologica Polonica*, 66(2), 409–423. 1400 https://doi.org/10.4202/app.00847.2020 1401 Mey, P. H. W., Nagtegaal, P. J. C., Roberti, K. J., & Hartevelt, J. J. A. (1968). 1402 Lithostratigraphic subdivision of post-Hercynian deposits in the south-central 1403 Pyrenees, Spain. Leidse Geologische Mededelingen, 41, 221–228. 1404 Mutti, E., & Sgavetti, M. (1987). Sequence stratigraphy of the Upper Cretaceous Aren 1405 strata in the Aren-Orcau region, south-central Pyrenees, Spain: Distinction 1406 between eustatically and tectonically controlled depositional sequences. Annali 1407 dell'Università di Ferrara, 1, 1–22. 1408 Nagtegaal, P. J. C., Van Vliet, A., & Brouwer, J. (1983). Syntectonic coastal offlap and 1409 concurrent turbidite deposition: The Upper Cretaceous Aren sandstone in the 1410 South-Central Pyrenees, Spain. Sedimentary Geology, 34, 185–218. https://

doi.org/10.1016/0037-0738(83)90086-6.

1411

- Novas, F. E. (1991). Relaciones filogeneticas de los dinosaurios teropodos
- 1413 ceratosaurios. *Ameghiniana*, 28(3–4), 410.
- Novas, F. E., Chatterjee, S., Rudra, D. K., & Datta, P. M. (2010). Rahiolisaurus
- 1415 *gujaratensis*, n. gen. n. sp., a new abelisaurid theropod from the Late Cretaceous
- of India. In S. Bandyopadhyay (Ed.). New Aspects of Mesozoic Biodiversity (pp.
- 1417 45–62). Springer.
- 1418 Novas, F. E., Agnolín, F. L., Ezcurra, M. D., Porfiri, J., & Canale, J. I. (2013).
- Evolution of the carnivorous dinosaurs during the Cretaceous: the evidence from
- 1420 Patagonia. Cretaceous Research, 45, 174–215.
- 1421 https://doi.org/10.1016/j.cretres.2013.04.001
- 1422 O'Connor, P. M. (2007). The postcranial axial skeleton of *Majungasaurus*
- 1423 *crenatissimus* (Theropoda: Abelisauridae) from the Late Cretaceous of
- 1424 Madagascar. Journal of Vertebrate Paleontology, 27(S2), 127-163.
- 1425 https://doi.org/10.1671/0272-4634(2007)27[127:TPASOM]2.0.CO;2
- 1426 Ortega, F., & Pérez-García, A. (2009). cf. *Lirainosaurus* sp. (Dinosauria: Titanosauria)
- en el Cretácico Superior de Sacedón (Guadalajara). *Geogaceta*, 46, 87–90.
- 1428 Ortega, F., Bardet, N., Barroso-Barcenilla, F., Callapez, P. M., Cambra-Moo, O.,
- Daviero-Gomez, V., Díez Díaz, V., Domingo, L., Elvira, A., Escaso, F., García-
- Oliva, M., Gomez, B., Houssaye, A., Knoll, F., Marcos-Fernandez, F., Martín, M.,
- Mocho, P., Narvaez, I., Perez-García, A., Peyrot, D., Segura, M., Serrano, H.,
- Torices, A., Vidal, D., & Sanz, J. L. (2015). The biota of the Upper Cretaceous
- site of Lo Hueco (Cuenca, Spain). *Journal of Iberian Geology*, 41, 83–99.
- 1434 https://doi.org/10.5209/rev_JIGE.2015.v41.n1.48657
- Ortega, F., Escaso, F., Mocho, P., Narváez, I., & Pérez-García, A. (2019). Eggs and
- bones: a preliminary comparison between the Upper Cretaceous faunas of the

1437 Poyos, Portilla and Lo Hueco sites (Villalba de la Sierra Formation. Central 1438 Spain). X Congreso Latinoamericano de Paleontología (p. 106). El Salvador. 1439 Ortega, F., Malafaia, E., Escaso, F., & Coria, R. A. (2022). New material of theropods 1440 (Abelisauroidea?) from Lo Hueco (Late Cretaceous, Cuenca, Central Spain). 1441 PalaeoVertebrata, special vol. 1, 147. https://doi.org/10.18563/pv.eavp2022 1442 Ősi, A., & Buffetaut, E. (2011). Additional non-avian theropod and bird remains from 1443 the early Late Cretaceous (Santonian) of Hungary and a review of the European 1444 abelisauroid record. Annales de Paléontologie, 97(1–2), 35–49. 1445 https://doi.org/10.1016/j.annpal.2011.07.001 1446 Ösi, A., Apesteguía, S., & Kowalewski, M. (2010). Non-avian theropod dinosaurs from 1447 the early Late Cretaceous of Central Europe. Cretaceous Research, 31(3), 304– 1448 320. https://doi.org/10.1016/j.cretres.2010.01.001 1449 Pereda-Suberbiola, X., & Sanz, J. L. (1999). The ornithopod dinosaur *Rhabdodon* from 1450 the Upper Cretaceous of Lano (Iberian peninsula). Museo de Ciencias naturales 1451 de Alava, 14(Número especial 1), 257–272. 1452 Pereda-Suberbiola, X., Astibia, H., Murelaga, X., Elorza, J. J., & Gómez-Alday, J. J. (2000). Taphonomy of the Late Cretaceous dinosaur-bearing beds of the Laño 1453 1454 Quarry (Iberian Peninsula). Palaeogeography, Palaeoclimatology, 1455 Palaeoecology, 157(3-4), 247-275. https://doi.org/10.1016/S0031-1456 0182(99)00169-8 1457 Pereda-Suberbiola, X., Corral, J. C., Astibia, H., Badiola, A., Bardet, N., Berreteaga, A., 1458 Buffetaut, E., Buscalioni, A. D., Cappetta, H., Cavin, L., Díez Díaz, V., 1459 Gheerbrant, E., Murelaga, X., Ortega, F., Pérez-García, A., Poyato-Ariza, F., 1460 Rage, J. C., Sanz, J. L., & Torices, A. (2015). Late cretaceous continental and 1461 marine vertebrate assemblages from the Laño quarry (Basque-Cantabrian Region,

1462 Iberian Peninsula): an update. *Journal of Iberian Geology*, 41, 101–124. 1463 https://doi.org/10.5209/rev_JIGE.2015.v41.n1.48658 1464 Pérez-García, A., Ortega, F., Bolet, A., Escaso, F., Houssaye, A., Martínez-Salanova, J., 1465 de Miguel Chaves, C., Mocho, P., Narvaez, I., Segura, M., Torices, A., Vidal, D., 1466 & Sanz, J. L. (2016). A review of the upper Campanian vertebrate site of Armuña 1467 (Segovia Province, Spain). Cretaceous Research, 57, 591–623. 1468 https://doi.org/10.1016/j.cretres.2015.08.008 1469 Pérez-García, A., Gascó, F., & Ortega, F. (2019). The Upper Cretaceous Poyos site: a 1470 large dinosaur nesting area in Central Spain. X Congreso Latinoamericano de 1471 Paleontología (p. 108). El Salvador. 1472 Pérez-García, A., Bardet, N., Fregenal-Martínez, M. A., Martín-Jiménez, M., Mocho, 1473 P., Narváez, I., Torices, A., Vullo, R., & Ortega, F. (2020). Cenomanian 1474 vertebrates from Algora (central Spain): New data on the establishment of the 1475 European Upper Cretaceous continental faunas. Cretaceous Research, 115, 104566. https://doi.org/10.1016/j.cretres.2020.104566 1476 1477 Pérez-Pueyo, M., Cruzado-Caballero, P., Moreno-Azanza, M., Vila, B., Castanera, D., Gasca, J. M., Puértolas-Pascual, E., Bádenas, B., & Canudo, J. I. (2021). The 1478 1479 Tetrapod Fossil Record from the Uppermost Maastrichtian of the Ibero-1480 Armorican Island: An Integrative Review Based on the Outcrops of the Western 1481 Tremp Syncline (Aragón, Huesca Province, NE Spain). Geosciences, 11(4), 1– 1482 162. https://doi.org/10.3390/geosciences11040162 1483 Platt, N. H. (1989). Lacustrine carbonates and pedogenesis: sedimentology and origin of 1484 palustrine deposits from the Early Cretaceous Rupelo Formation, W Cameros 1485 Basin, N Spain. Sedimentology, 36(4), 665–684. https://doi.org/10.1111/j.1365-

1486

3091.1989.tb02092.x

1487	Platt, N. H., & Wright, V. P. (1992). Palustrine carbonates and the Florida Everglades;
1488	towards an exposure index for the fresh-water environment?. Journal of
1489	Sedimentary Research, 62(6), 1058–1071. https://doi.org/10.1306/D4267A4B-
1490	2B26-11D7-8648000102C1865D
1491	Peyrot, D., Barron, E., Pereda-Suberbiola, X., & Company, J. (2020). Vegetational
1492	composition of the Upper Cretaceous vertebrate site of Chera (Valencia, Spain)
1493	and its significance in mosaic vegetation from southwestern Europe. Cretaceous
1494	Research, 106, 104254. https://doi.org/10.1016/j.cretres.2019.104254
1495	Pol, D., & Rauhut, O. W. M. (2012). A Middle Jurassic abelisaurid from Patagonia and
1496	the early diversification of theropod dinosaurs. Proceedings of the Royal Society
1497	B, 279(1741), 3170–3175. https://doi.org/10.1098/rspb.2012.0660
1498	Puértolas-Pascual, E., Arenillas, I., Arz, J. A., Calvín, P., Ezquerro, L., García-Vicente,
1499	C., Pérez-Pueyo, M., Sánchez-Moreno, E. M., Villalaín, J. I., & Canudo, J. I.
1500	(2018). Chronostratigraphy and new vertebrate sites from the upper Maastrichtian
1501	of Huesca (Spain), and their relation with the K/Pg boundary. Cretaceous
1502	Research, 89, 36–59. https://doi.org/10.1016/j.cretres.2018.02.016
1503	Rauhut, O. W. M. (2003). The interrelationships and evolution of basal theropod
1504	dinosaurs. Special Papers in Palaeontology, 69, 1–213.
1505	Richter, U., Mudroch, A., & Buckley, L. G. (2013). Isolated theropod teeth from the
1506	Kem Kem beds (early Cenomanian) near Taouz, Morocco. Paläontologische
1507	Zeitschrift, 87, 291–309. https://doi.org/10.1007/s12542-012-0153-1
1508	Rosell, J., Linares, R., & Llompart, C. (2001). El "Garumniense" prepirenaico. Revista
1509	de la Sociedad Geológica de España, 14, 47–56.

1510 Ruiz-Omeñaca, J. I., Vullo, R., Bernárdez, E., & Buscaloni, Á. D. (2009). El primer 1511 resto directo de terópodo del Cenomaniense de la Peninsula Ibérica: el diente de 1512 Limanes (Oviedo, Asturias). Geogaceta, 47(3-4), 29–32. 1513 Sales, M. A., Lacerda, M. B., Horn, B. L., de Oliveira, I. A., & Schultz, C. L. (2016). The " χ " of the matter: testing the relationship between paleoenvironments and 1514 1515 three theropod clades. *PLOS ONE*, 11(2), e0147031. 1516 https://doi.org/10.1371/journal.pone.0147031 1517 Santos Brilhante, N., de França, T. C., Castro, F., Sanches da Costa, L., Currie, P. J., 1518 Kugland de Azevedo, S. A., & Delcourt, R. (2022). A dromaeosaurid-like claw 1519 from the Upper Cretaceous of southern France. Historical Biology, 34(11), 2195– 1520 2204. https://doi.org/10.1080/08912963.2021.2007243 1521 Sauvage, H. E. (1897–1898). Fossil vertebrates from Portugal. Contributions to the 1522 study of fish and reptiles from the Jurassic and Cretacic. Direction des Travaux 1523 Géologiques du Portugal, 29, 1–46. 1524 Serrano-Martínez, A., Ortega, F., Sciscio, L., Tent-Manclús, J. E., Fierro Bandera, I., & 1525 Knoll, F. (2015). New theropod remains from the Tiouraren Formation (?Middle 1526 Jurassic, Niger) and their bearing on the dental evolution in basal tetanurans. *Proceedings of the Geologists' Association*, 126(1), 107–118. 1527 1528 https://doi.org/10.4202/app.00101.2014. 1529 Smith, J. B. (2007). Dental morphology and variation in *Majungasaurus crenatissimus* 1530 (Theropoda: Abelisauridae) from the Late Cretaceous of Madagascar. Society of 1531 *Vertebrate Paleontology Memoir*, 8, 103–126. 1532 Smith, J. B., & Dodson, P. (2003). A proposal for a standard terminology of anatomical 1533 notation and orientation in fossil vertebrate dentitions. Journal of Vertebrate

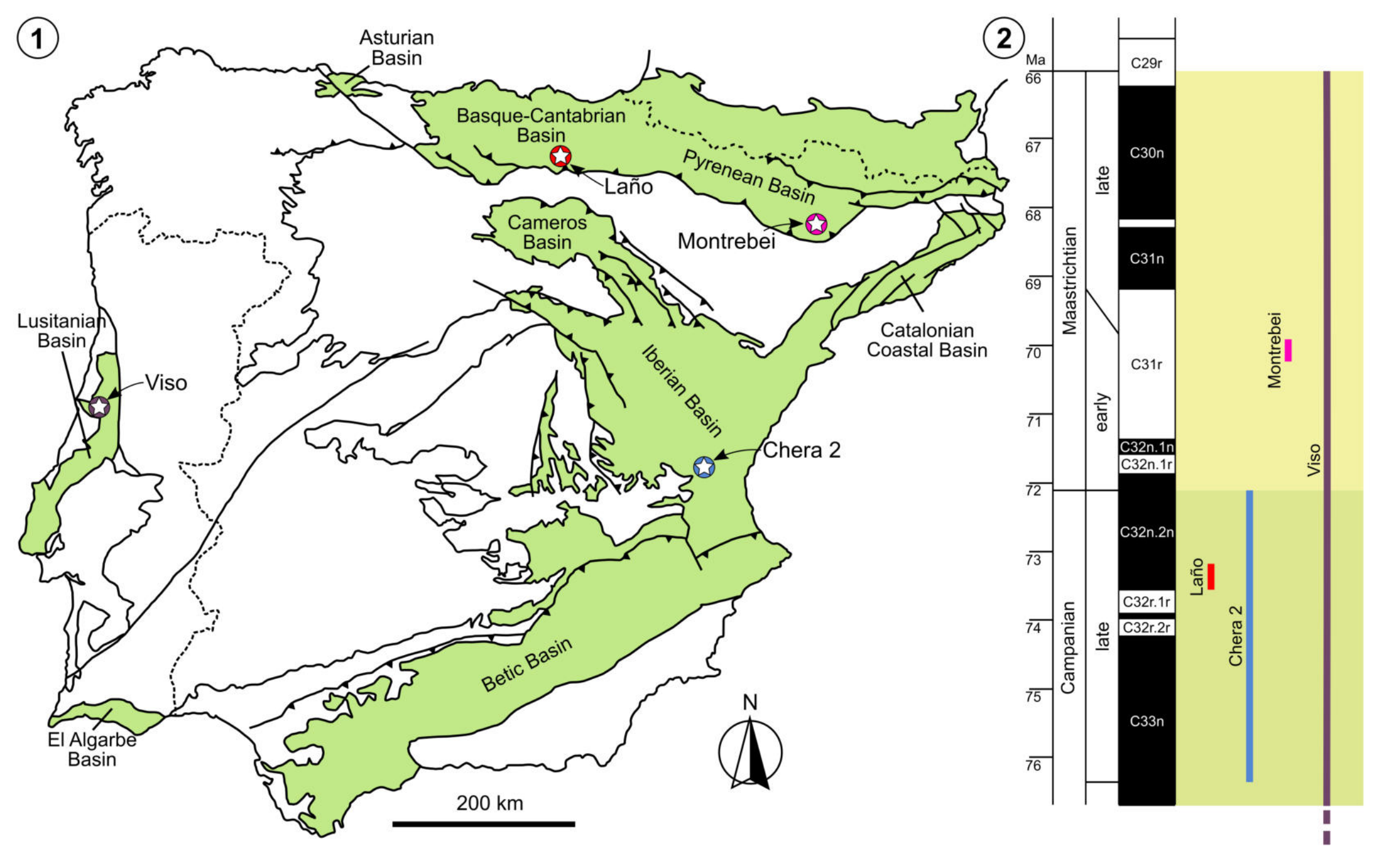
1534 paleontology, 23(1), 1–12. https://doi.org/10.1671/0272-1535 4634(2003)23[1:APFAST]2.0.CO;2 Smith, J. B., Vann, D. R., & Dodson, P. (2005). Dental morphology and variation in 1536 1537 theropod dinosaurs: implications for the taxonomic identification of isolated teeth. 1538 The Anatomical Record Part A: Discoveries in Molecular, Cellular, and 1539 Evolutionary Biology: An Official Publication of the American Association of 1540 Anatomists, 285(2), 699–736. https://doi.org/10.1002/ar.a.20206 1541 Soto, M., Delcourt, R., Langer, M. C., & Perea, D. (2022). The first record of 1542 Abelisauridae (Theropoda: Ceratosauria) from Uruguay (Late Jurassic, 1543 Tacuarembó Formation). *Historical Biology*, 35(12), 2362–2371. 1544 https://doi.org/10.1080/08912963.2022.2140425 1545 Torices Hernández, A. (2002). Los dinosaurios terópodos del Cretácico Superior de la 1546 Cuenca de Tremp (Pirineos Sur-Centrales, Lleida). Coloquios de Paleontología, 1547 *53*, 139–146. 1548 Torices, A., Barroso-Barcenilla, F., Cambra-Moo, O., Pérez-García, A., & Segura, M. 1549 (2012). Palaeontological and palaeobiogeographical implications of the new 1550 Cenomanian vertebrate site of Algora, Guadalajara, Spain. Cretaceous Research, 1551 37, 231–239. https://doi.org/10.1016/j.cretres.2012.04.004 1552 Torices, A., Currie, P. J., Canudo, J. I., & Pereda-Suberbiola, X. (2015). Theropod 1553 dinosaurs from the upper cretaceous of the south pyrenees basin of Spain. Acta 1554 Palaeontologica Polonica, 60(3), 611–626. https://doi.org/10.4202/app.2012.0121 1555 Tortosa, T., Buffetaut, E., Vialle, N., Dutour, Y., Turini, E., & Cheylan, G. (2014). A new abelisaurid dinosaur from the Late Cretaceous of southern France: 1556 1557 Palaeobiogeographical implications. Annales de Paleontologie, 100(1), 63–86. 1558 https://doi.org/10.1016/j.annpal.2013.10.003

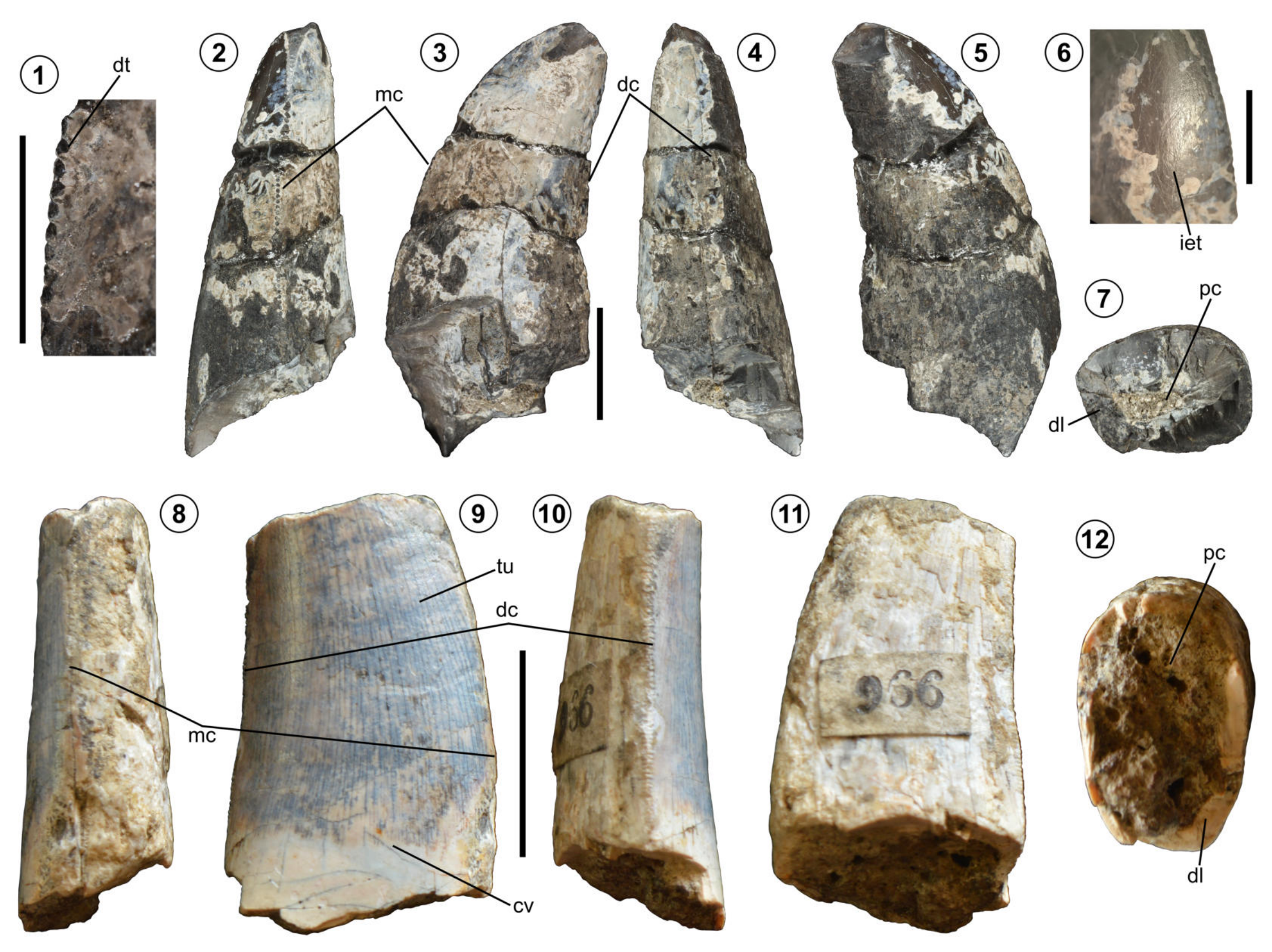
1559	Valentin, X., Godefroit, P., Tabuce, R., Vianey-Liaud, M., Wu, W., & García, G.,
1560	(2012). First late Maastrichtian (latest Cretaceous) vertebrate assemblage from
1561	Provence (Vitrolles-la-Plaine, southern France). In P. Godefroit, (Ed.). Bernissart
1562	Dinosaurs and Early Cretaceous Terrestrial Ecosystems (pp. 582-597). Indiana
1563	University Press.
1564	Vicente, A., Villalba Breva, S., Ferràndez-Cañadell, C., & Martín-Closas, C. (2014).
1565	Revision of the Maastrichtian-Palaeocene charophyte biostratigraphy of the
1566	Fontllonga reference section (southern Pyrenees, Catalonia, Spain). Geologica
1567	Acta, 14(4), 349–362. https://doi.org/10.1344/GeologicaActa2016.14.4.2
1568	Vicente, A., Martín-Closas, C., Arz, J. A., & Oms, O. (2015). Maastrichtian-basal
1569	Paleocene charophyte biozonation and its calibration to the Global Polarity Time
1570	Scale in the southern Pyrenees (Catalonia, Spain). Cretaceous Research, 52(A),
1571	268–285. https://doi.org/10.1016/j.cretres.2014.10.004
1572	Vullo, R., Neraudeau, D., & Lenglet, T. (2007). Dinosaur teeth from the Cenomanian of
1573	Charentes, western France: evidence for a mixed Laurasian-Gondwanan
1574	assemblage. Journal of Vertebrate Paleontology, 27(4), 931–943.
1575	https://doi.org/10.1671/0272-4634(2007)27[931:DTFTCO]2.0.CO;2
1576	Wilson, J. A., Sereno, P. C., Srivastava, S., Bhatt, D. K., Khosla, A., & Sahni, A.
1577	(2003). A new abelisaurid (Dinosauria Theropoda) from the Lameta Formation
1578	(Cretaceous, Maastrichtian) of India. Contributions from the Museum of
1579	Paleontology. University of Michigan, 31(1), 1–42.
1580	
1581	Appendices
1582	Supplementary material 1. Measurements of the studied teeth, datasets, and DA
1583	reculto

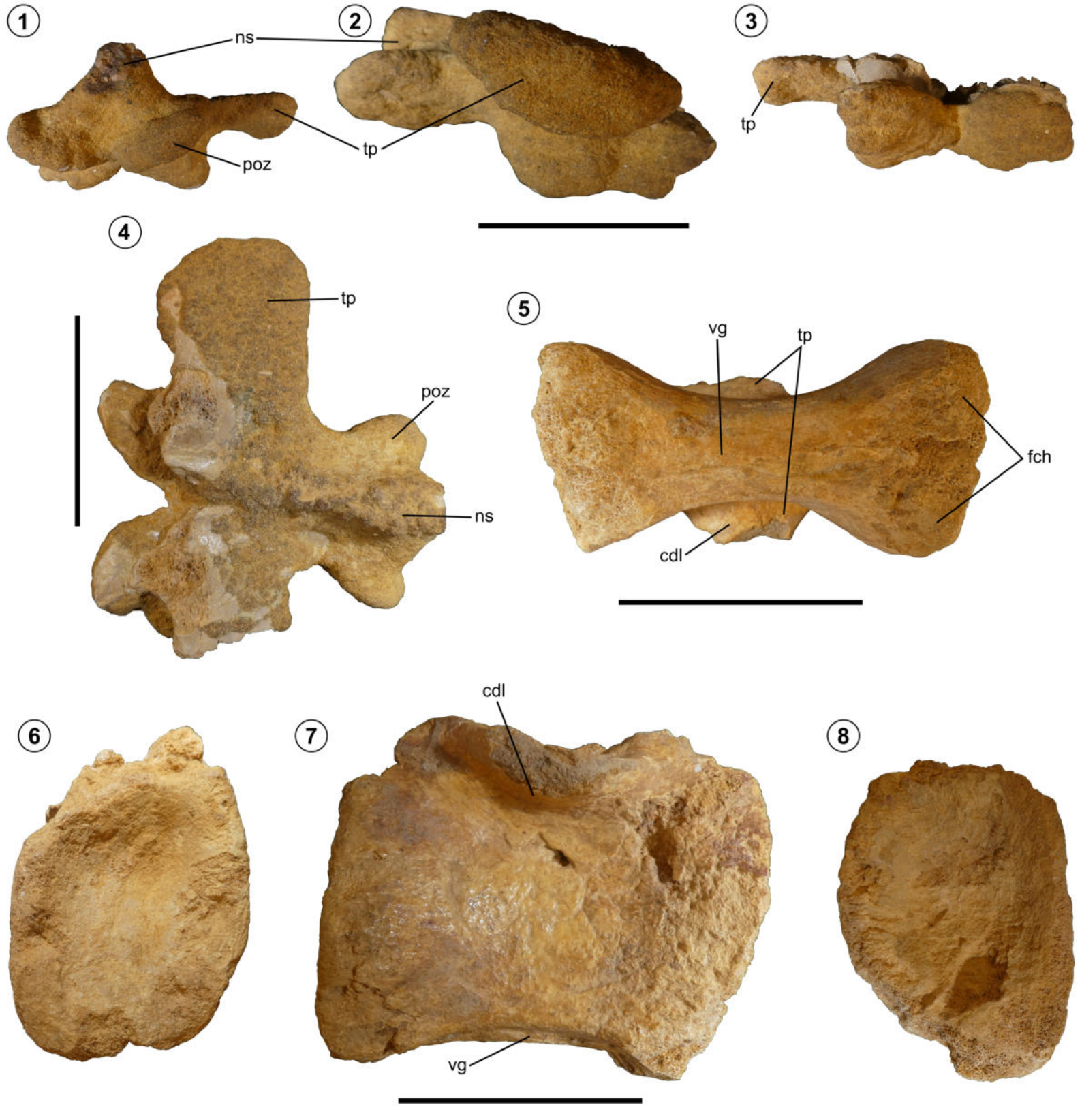
- 1584 **Supplementary material 2.** Nexus file of the dental matrix.
- 1585 **Supplementary material 3.** Abelisauridae and possible Abelisauridae occurrences and
- 1586 locality list for the Upper Cretaceous of the Ibero-Armorican Domain.
- 1587 Figure captions
- 1588 **Figure 1.** Geologic and chronostratigraphic setting of the uppermost Cretaceous fossil
- sites where the studied remains were recovered. 1, map of the Iberian Mesozoic basins
- showing the locations of the Chera 2, Laño, Montrebei, and Viso fossil sites (modified
- 1591 from Gómez et al., 2019); and 2, chronostratigraphic position of the Chera 2, Laño,
- 1592 Montrebei and Viso fossil sites.
- 1593 **Figure 2.** Abelisauridae indet. teeth from Montrebei and Viso. Morphotype 1 (**DPM**-
- 1594 MON-T10 1) 1, mesial denticles; crown in 2, mesial; 3, lingual; 4, distal; and 5, labial
- views; 6, close up of enamel texture; and 7, basal cross section in basal view.
- Morphotype 2 (MG 73) tooth in 8, mesial; 9, lingual; 10, distal; 11, labial; and 12, basal
- views (modified from Malafaia et al., 2024). Abbreviations: cv, cervix; dt, denticle; mc,
- mesial carina; **dc**, distal carina; **dl**, dentine layer; **iet**, irregular enamel texture; **pc**, pulp
- cavity; tu; transverse undulation. Scale bar equals 1 cm, except for denticles and texture
- 1600 (5 mm).
- 1601 **Figure 3.** cf. *Arcovenator* axial elements from Laño. Anterior dorsal vertebra (MCNA
- 1602 8366) in 1, posterior; 2, lateral; 3, anterior; and 4; dorsal views. Caudal vertebra
- 1603 (MCNA 17433) in 5, ventral; 6, anterior; 7, lateral; and 8, posterior views.
- Abbreviations: **cdl**, centrodiapophyseal lamina; **fch**, facet for chevron; **ns**, neural spine;
- poz, postzygapophysis; tp, transverse process; vg, ventral groove. Scale bar equals 5
- 1606 cm.
- 1607 **Figure 4.** Arcovenator sp. tooth from Chera 2 (**CH** 168). 1, mesial denticles; crown in
- 1608 2, mesial; 3, lingual; 4, distal; 5, labial; and 6, basal views. 7, close up of enamel

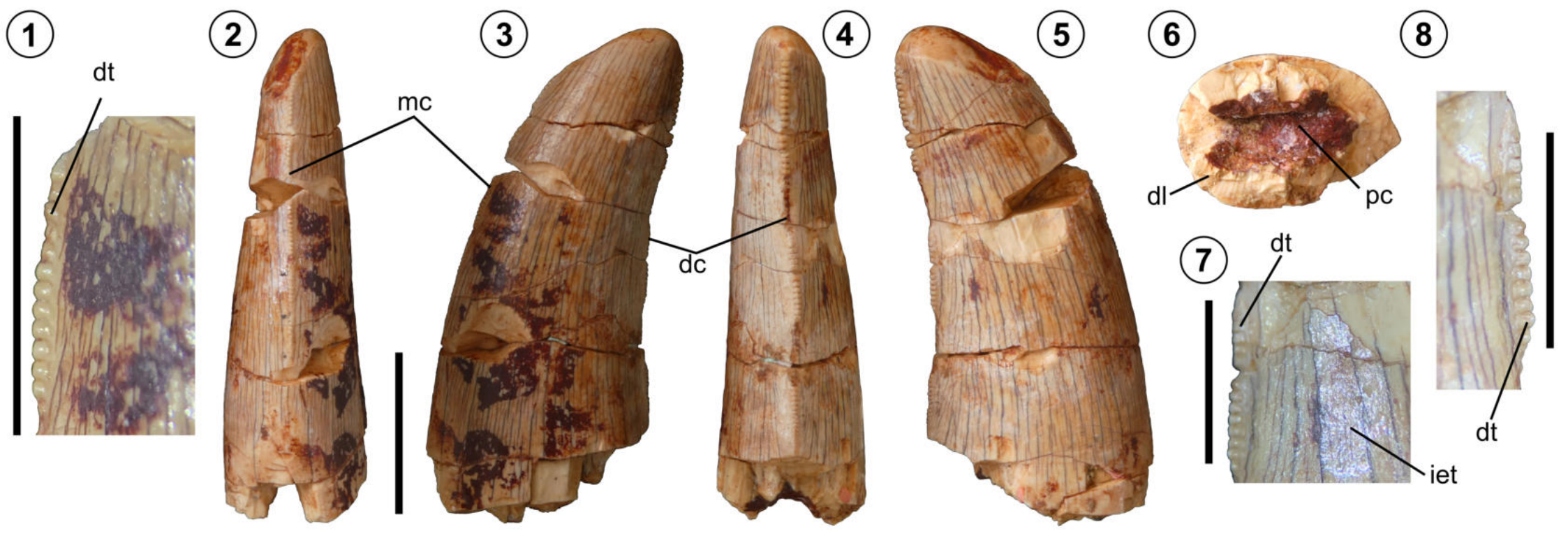
- 1609 texture; and **8**, distal denticles. Abbreviations: **dt**, denticle; **mc**, mesial carina; **dc**, distal
- carina; **dl**, dentine layer; **iet**, irregular enamel texture; **pc**, pulp cavity. Scale bar equals 1
- 1611 cm, except for denticles and texture (5 mm).
- 1612 **Figure 5.** Graphical results of the LDAs (LDA 1 and 3) carried out at the clade-level. **1**,
- LDA performed using database 1 at clade-level. Axis 1 accounts for 47.67 % of the
- variance (Eigenvalue = 2.6735), and Axis 2 accounts for 24.67 % of the variation
- 1615 (Eigenvalue = 1.3703). **2**, LDA performed using database 2 at the clade-level. Axis 1
- accounts for 55.62 % of the variance (Eigenvalue = 2.6056), and Axis 2 for 30.06 % of
- 1617 the variation (Eigenvalue = 1.4081). Silhouettes courtesy of Scott Hartman.
- 1618 **Figure 6.** Graphical results of the LDA performed with the Ibero-Armorican abelisaurid
- teeth (database 3). Axis 1 accounts for 49.29 % of the variance (Eigenvalue = 2.8359),
- and Axis 2 for 26.72 % of the variation (Eigenvalue = 1.5371).
- 1621 Figure 7. Results of the phylogenetic analyses performed for specimens MG 73 and
- 1622 **CH** 168 based on the dentition-based data matrix (constrained search) of Hendrickx et
- 1623 al. (2020). **1,** simplified single MPT (CI = 0.203; RI = 0.542) obtained from the
- phylogenetic analysis, showing the position of specimen MG 73 from Viso (highlighted
- in bold). 2, simplified consensus tree (CI = 0.199; RI = 0.452) obtained from five MPTs
- recovered in the phylogenetic analysis, showing the position of specimen CH 168 from
- 1627 Chera 2 (highlighted in bold).
- 1628 **Figure 8.** Simplified strict consensus tree (CI = 0.1809; RI = 0.376) obtained from
- seven MPTs recovered in the phylogenetic analysis based on the dentition-based data
- matrix (constrained search) of Hendrickx et al. (2020), showing the position of **DPM**-
- 1631 **MONT-T1** 1 from Montrebei (highlighted in bold).
- 1632 **Figure 9.** Paleogeographic and temporal distribution of the currently known Ibero-
- Armorican abelisaurids and large-sized theropod remains that likely belong to

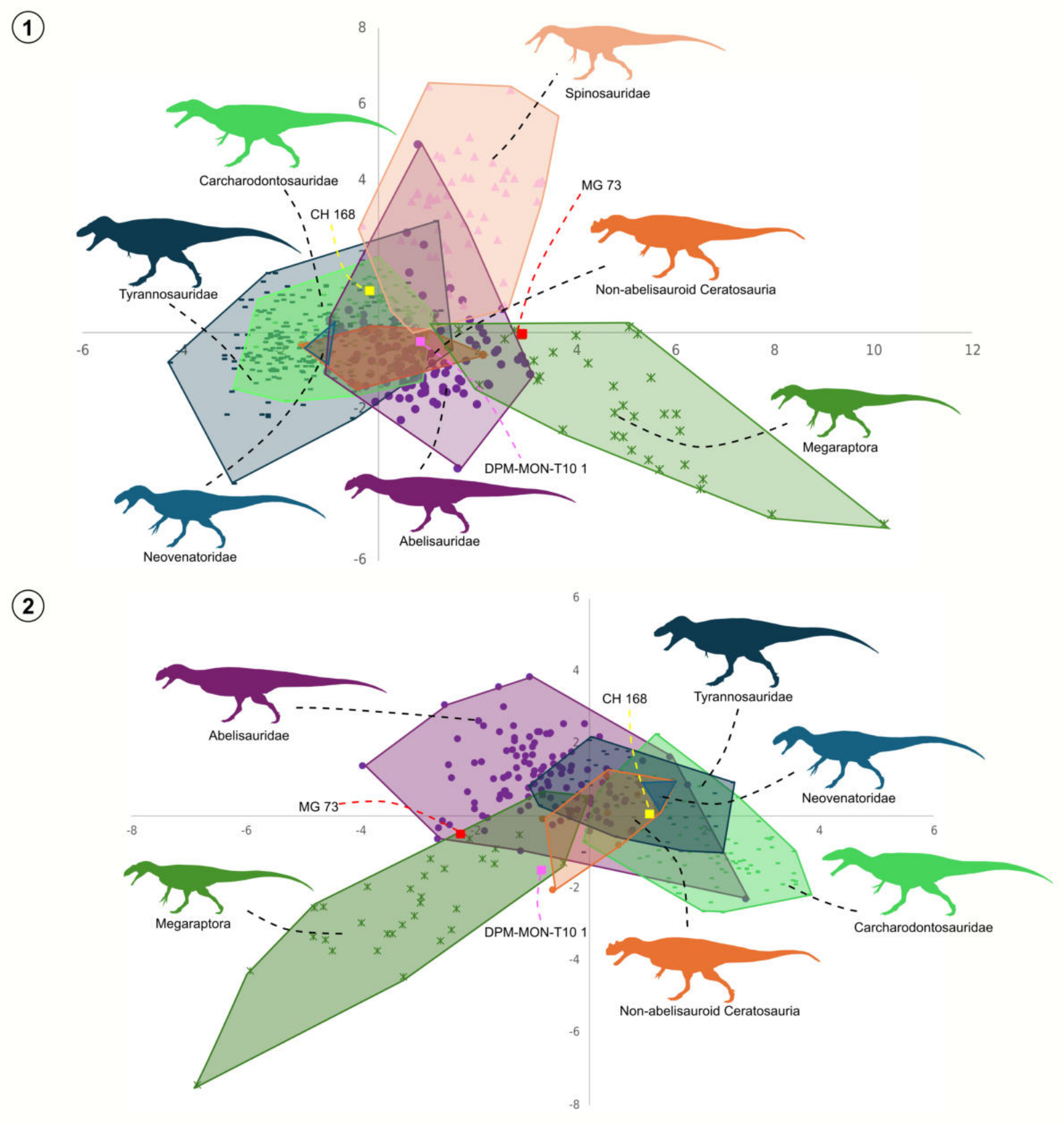
1634	Abelisauridae. 1, map of the Ibero-Armorican Mesozoic basins (modified from
1635	Buffetaut et al., 2024; Malafaia et al., 2025) showing the location where Late
1636	Cretaceous Ibero-Armorican abelisaurid or large-sized theropod remains have been
1637	recovered. 2, chronological distribution of the Late Cretaceous abelisaurids or large-
1638	sized theropods that may be identified as Abelisauridae (modified from Tortosa et al.,
1639	2014). Abelisaurid- or large-size theropod-bearing sites or areas: 1, Saint-Jouin-
1640	Bruneval; 2, "La Buzinie"; 3, Limanes; 4, Algora; 5, Viso; 6, Lambeau du Beausset; 7,
1641	Trets-La Boucharde; 8, Velaux-La Bastide Neuve; 9, Fox-Amphoux; 10, Pourrières-Jas
1642	Neuf Sud; 11, Laño; 12, Armuña; 13, Chera 2; 14, Cruzy; 15, Pourcieux-Les Tuillières;
1643	16, Cassagnau 1; 17, Lo Hueco; 18, Poyos; 19, Vitrolles-La Plaine; 20, Montrebei; 21,
1644	Blasi; 22, 172-i/04/e.
1645	

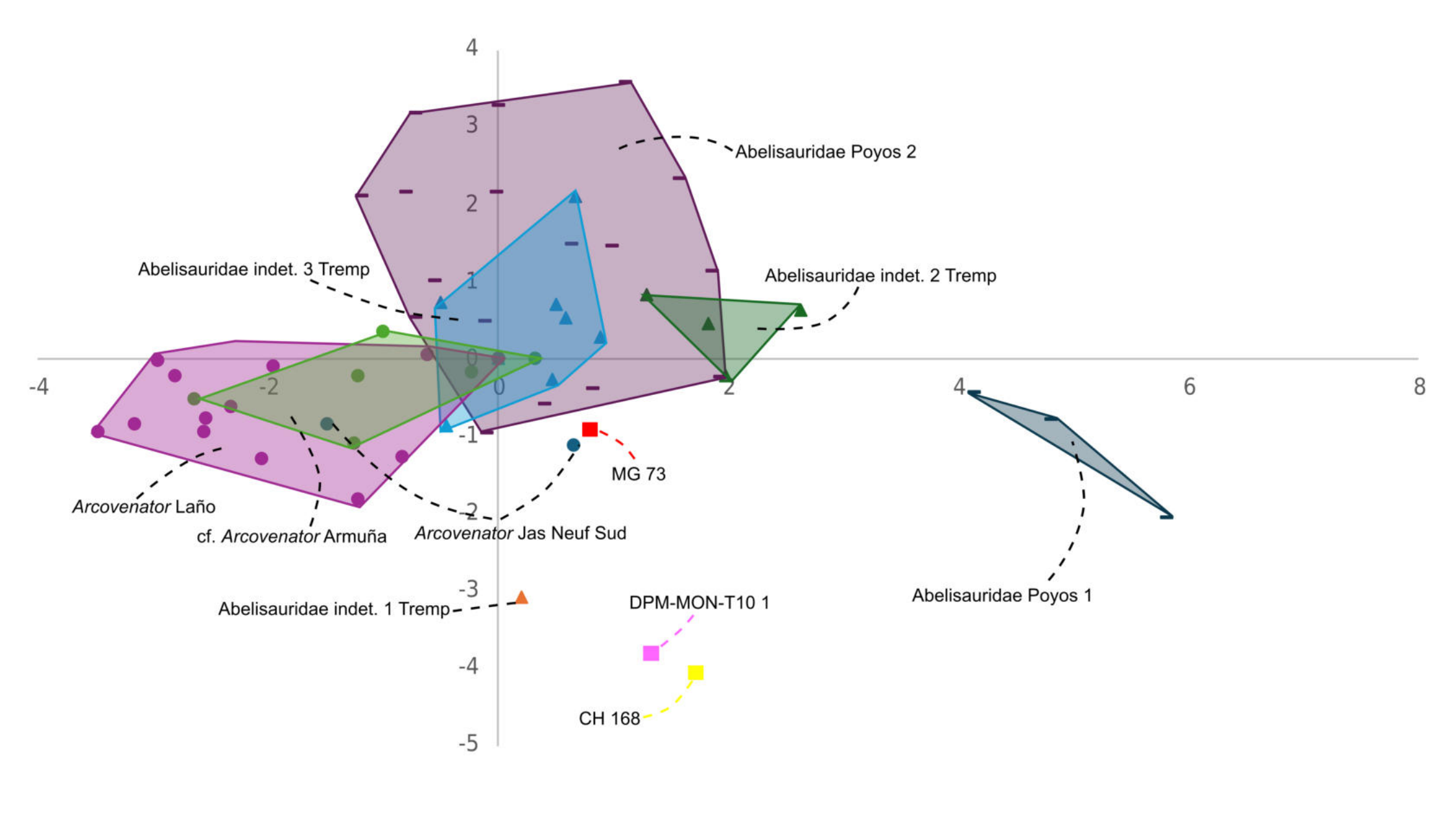


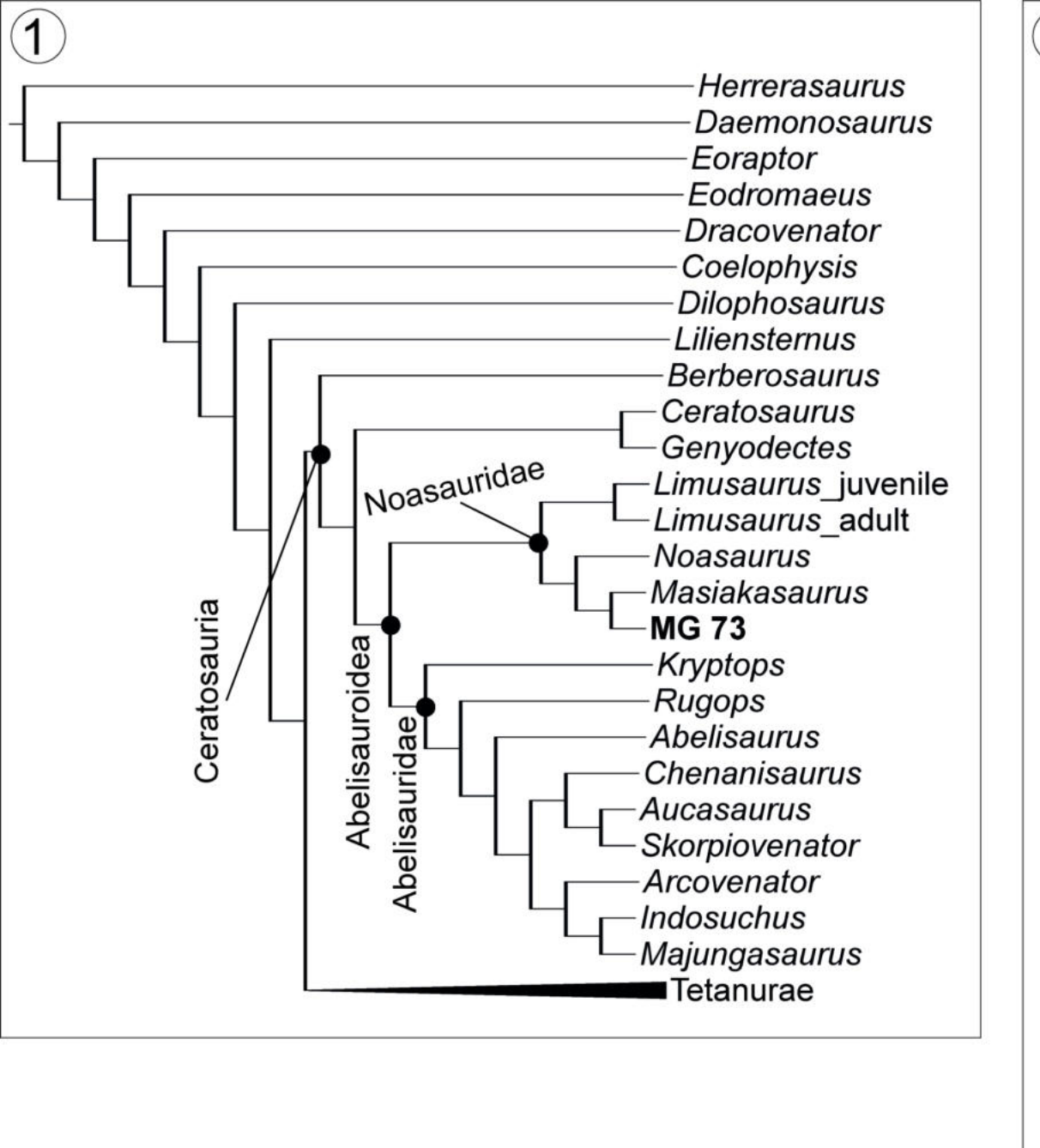


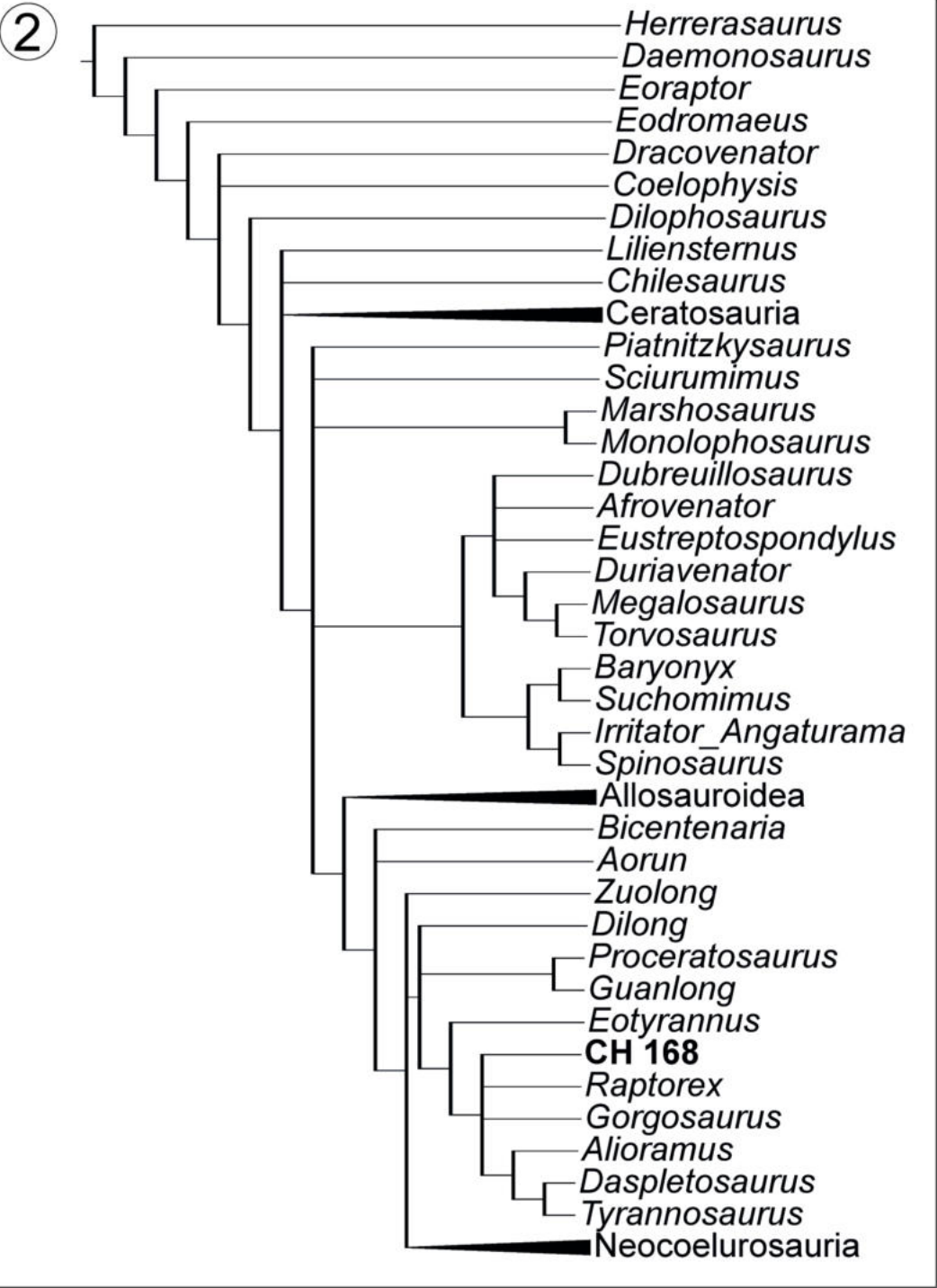


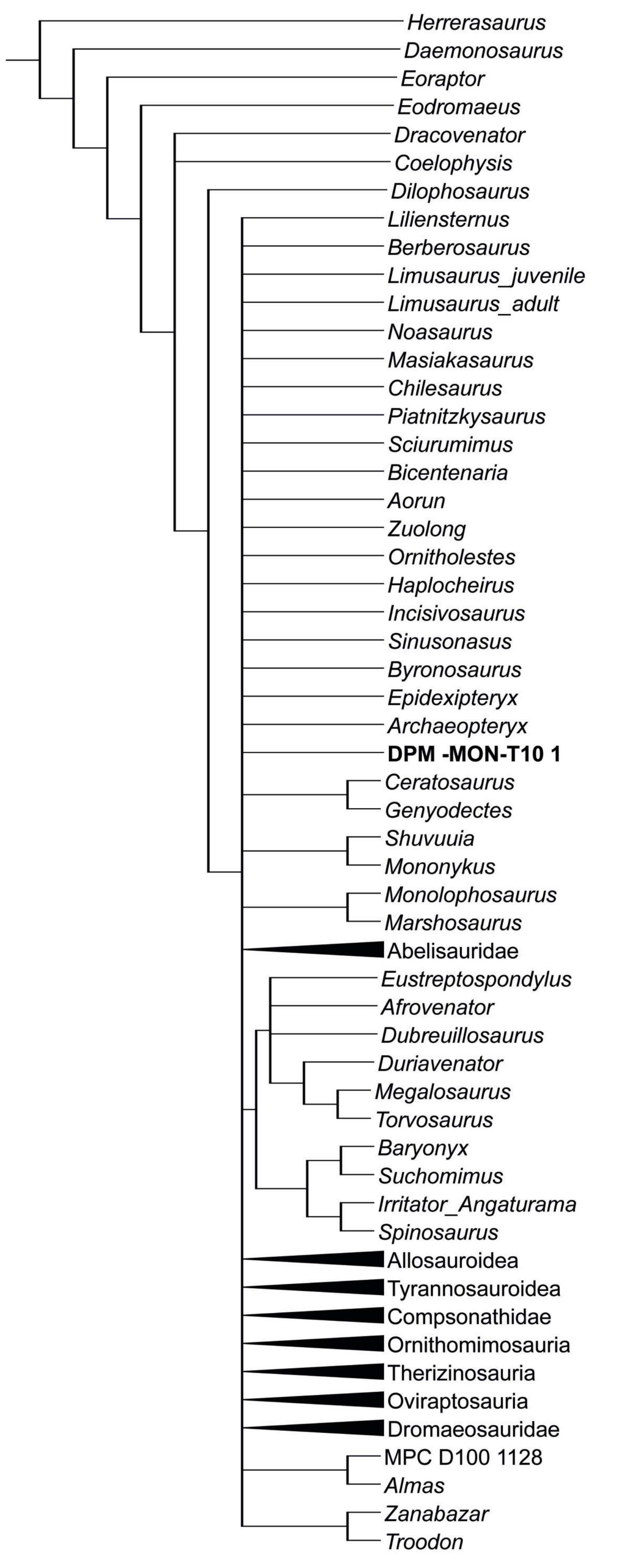












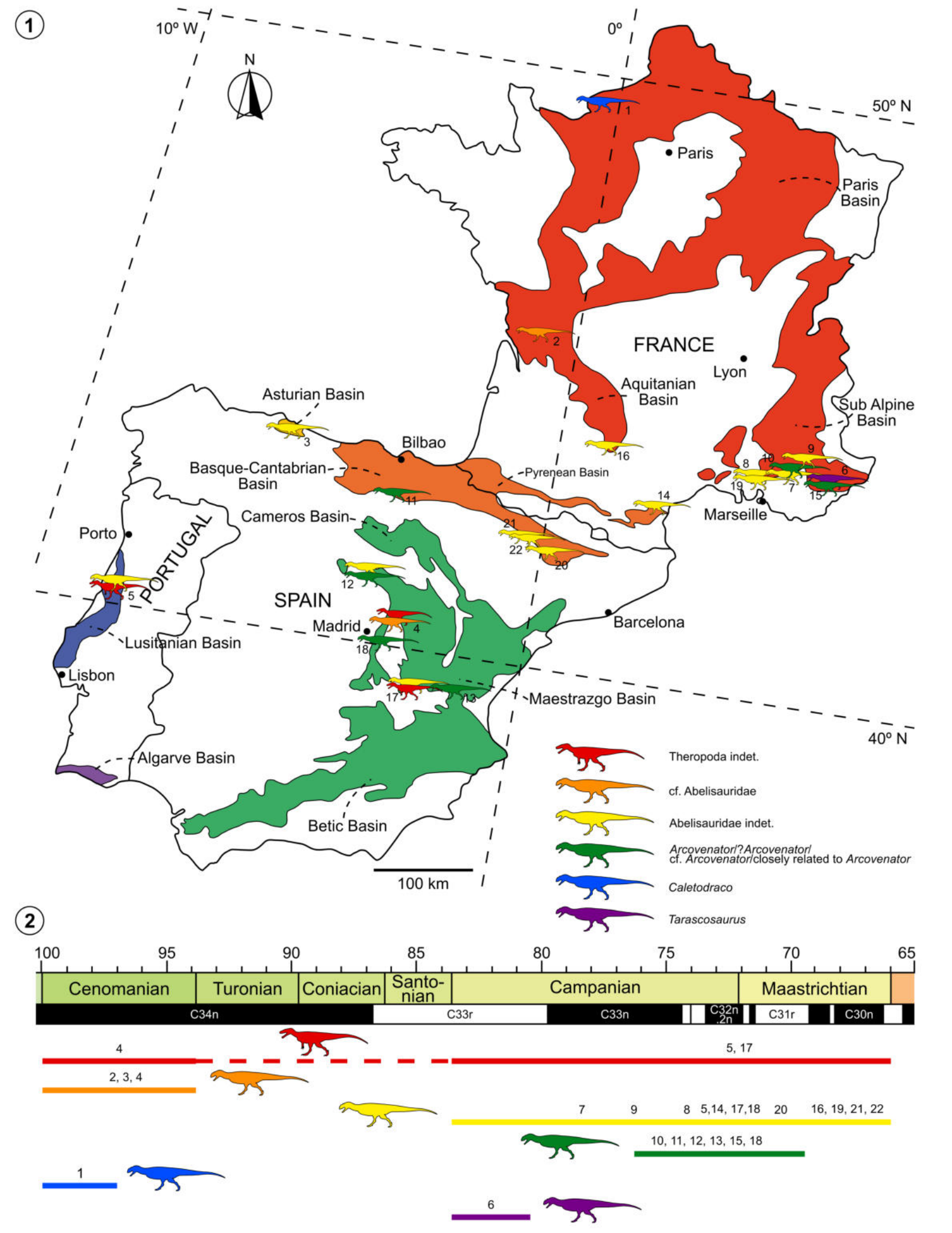


TABLE 1. Results of the discriminant analyses performed with database 1, 2 and 3. Databases in Supplementary material 1.

	LDA 1 (clade)		LDA 2 (taxa)		LDA 3 (clade)		LDA 4 (taxa)		LDA 5 (Ibero- armorica)	
	Classifica tion	Jackknif ed	Classifi cation	Jackkni fed	Classif ication	Jackkn ifed	Class ificati on	Jackk nifed	Class ificati on	Jackk nifed
M G 73		Abelisau ridae	Carnot aurus	Carnot aurus		Megar aptora	Carn otaur us	Carn otaur us	Arcov enato r Jas Neuf Sud	Arcov enato r Jas Neuf Sud
C H 16 8		Non- abelisaur oid Ceratosa uria		Gorgos aurus	Tyrann osauri dae	Tyrann osauri dae		Gorg osaur us	Suu	Abeli sauri dae indet. closel y relate d to Arcov enato r Poyo s. Morp hotyp e 1
D P M - M O N- T1 0	Carcharo dontosaur idae	Carcharo dontosau riae	Acroca nthosau rus	Acroca nthosau rus		Megar aptora	Auca sauru s	Auca sauru s		Abeli sauri dae indet. 1 West ern Trem p Syncl ine